ARISTOTLE UNIVERSITY OF THESSALONIKI
Interinstitutional Program of Postgraduate Studies in
PALAEONTOLOGY – GEOBIOLOGY

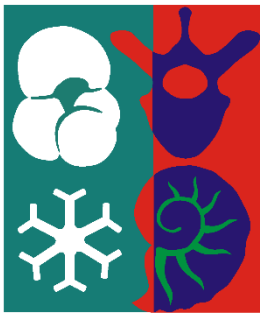

ANASTASIOS NIKITAS
Geologist, MSc

Olimpi mud volcanoes sedimentary records (Hellenic arc): geochemical and micropaleontological characterization

MASTER THESIS

DIRECTION: Micropalaeontology-Biostratigraphy
Directed by: National & Kapodistrian University of Athens

ATHENS,
2020

Interinstitutional
Program of
Postgraduate
Studies in
PALAEONTOLOGY – GEOBIOLOGY

supported by:

Τμήμα Γεωλογίας ΑΠΘ
School of Geology AUTh

Τμήμα Βιολογίας ΑΠΘ
School of Biology AUTh

National and
Kapodistrian
University of
Athens
Faculty of Geology and
Geoenvironment

Τμήμα Γεωλογίας & Γεωπεριβάλλοντος
ΕΚΠΑ
Faculty of Geology & Geoenvironment
NKUA

Department of GEOLOGY

Τμήμα Γεωλογίας Παν/μίου Πατρών
Department of Geology, Patras Univ.

UNIVERSITY OF THE AEGEAN

Τμήμα Γεωγραφίας Παν/μίου Αιγαίου
Department of Geography, Aegean
Univ.

ANASTASIOS NIKITAS
ΑΝΑΣΤΑΣΙΟΣ ΝΙΚΗΤΑΣ
Πτυχιούχος τμήματος Γεωλογίας ΑΠΘ,
Πτυχιούχος Μεταπτυχιακού ‘’Έρευνα και Εκμετάλλευση Υδρογονανθράκων’’, ΑΠΘ

Olimpi mud volcanoes sedimentary records (Hellenic arc): geochemical and micropaleontological characterization

Ιζηματολογική καταγραφή του πεδίου λασποηφαιστείων Olimpi (Ελληνικό Τόξο): γεωχημικός και μικροπαλαιοντολογικός χαρακτηρισμός

Υποβλήθηκε στο ΔΠΜΣ Παλαιοντολογία-Γεωβιολογία

Ημερομηνία Προφορικής Εξέτασης: 28/02/2020
Oral Examination Date: 28/02/2020

Three-member Examining Board

Dr. Alexandra Gogou, Supervisor
Professor Maria V. Triantaphyllou, Member
Dr. Grigoris Rousakis, Member

Τριμελής Εξεταστική Επιτροπή

Δρ. Αλεξάνδρα Γώγου, Επιβλέπων
Καθηγήτρια Τριανταφύλλου Μαρία, Μέλος Τριμελούς Εξεταστικής Επιτροπής
Δρ. Γρηγόρης Ρουσάκης, Μέλος Τριμελούς Εξεταστικής Επιτροπής

Olimpi mud volcanoes sedimentary records (Hellenic arc): geochemical and micropaleontological characterization – *Master Thesis*

Ιζηματολογική καταγραφή του πεδίου λασποηφαιστείων Olimpi (Ελληνικό Τόξο): γεωχημικός και μικροπαλαιοντολογικός χαρακτηρισμός – *Μεταπτυχιακή Διπλωματική Εργασία*

Citation:
Nikitas A., 2020. – Olimpi mud volcanoes sedimentary records (Hellenic arc): geochemical and micropaleontological characterization, Interinstitutional Program of Postgraduate Studies in Palaeontology-Geobiology. School of Geology, Aristotle University of Thessaloniki, 70 pp.

Table of Contents

Acknowledgments

I would like thank Dr. Alexandra Gogou, Dr. Ioannis Panagiotopoulos and Dr. Grigoris Rousakis for providing me the chance to study the cores recovered during LEVECO cruise (2016). I also thank them for their precious advices.

I would like to thank Professor Maria V. Triantaphyllou for her precious guidelines and advice during the calcareous nannoplankton study and her general support during this master thesis.

I would like to thank Professor Nikos Pasadakis for conducting the Rock Eval pyrolysis, which added great value to this master thesis.

Lastly, I would like to thank all my colleagues and professors in the Interinstitutional Program of Postgraduate Studies ''PALAEONTOLOGY – GEOBIOLOGY'' for all the new knowledge and experience that I have gained.

Abstract

This master thesis produces scientific information concerning the mud breccia extruded from five (5) mud volcanoes of the Olimpi MV field (Mediterranean Ridge). In total, 42 samples (14 mud breccia matrix and 28 clasts samples) were retrieved and studied. Routine micropaleontological (calcareous nannoplankton) analysis has been performed in order to determine the possible age of the deep-seated source strata. In addition, for the first time, the total organic carbon and thermal maturity of samples recovered from deep (sub-salt) layers of the Mediterranean Ridge were determined through organic geochemical study (Rock-Eval pyrolysis) and an attempt to evaluate the oil and gas potential of the sediments has been made. It is concluded that: (1) mudstone/shale clasts of different stratigraphic position were found and attributed to biozones NN7, NN6, NN5, NN4 and NP24, (2) some samples showed a heavy mixing of Miocene and Oligocene nannofossils while others appeared to be barren of nannofossils and consequently could not be dated, (3) samples appeared to be both organic rich (TOC>0.5) and poor (TOC<0.5), mostly comprised of Type III kerogen which is considered immature – nearly mature, with respect to gas and/or oil generation and poor to fair generative potential and (4) a single mudstone clast attributed to NN7 showed a completely different micropaleontological and geochemical image and is considered as of sapropelic origin. The above information seems to confirm and add more information in the S-SW orogen migration theory.

Introduction

Mud volcanic structures are very common along the eastern Mediterranean seafloor, distributed in areas being under compressional regime. In total, more than 250 MV structures have been identified in the Mediterranean Ridge, while such structures are absent through the neighboring backstop area which is tectonically inactive or even under extensional regime at places. Mud volcanoes are considered the most important pathway for the release of pressure caused by predominantly tectonic movements and secondary by the production of diagenetic fluids (biogenic and/or thermogenic) in deep seated sediments. Dimitrov (2002) attempted to quantify the total methane releases from mud volcanoes and proposed that emits can fluctuate between 10.3–12.6 Tg/year (1 Tg=1 million tons).

Many studies have been conducted through the past decades concerning the mud volcanoes' spatial distribution (Limonov et al., 1996; Fusi et al., 1996; Cita et al., 1989; Leité & Mascle, 1982; Rabaute & Chamot-Rooke, 2007; Mascle et al., 2014), sedimentological and geochemical characteristics (Emeis et al., 1996; Akhmanov et al., 1996; Schulz et al. 1997; Kopf et al., 2000) and their possible relation to gas hydrates and gas seeps (Aloisi et al., 2000; Woodside et al., 1998; Woodside et al., 1997; Perissoratis et al., 2011; Pape et al., 2010).

Experience from the Mediterranean Sea, has shown that sediments extruded from mud volcanoes comprise of a mixture of poorly sorted clayey, silty and sandy material along with angular to round coarser grains (e.g. pebbles, cobbles or even larger material), that usually do not share the same stratigraphic origin. The established description for these sediments is "mud breccia''. Cita et al. (1981), were the first to use the term "mud breccia'' in order to describe the material extruded to the surface of Prometheus Dome, which comprise of a grey clay and silt-sized matrix, supporting

centimeter-size sub-rounded clasts of semi-indurated sediment (Camerlenghi et al., 1992).

The Olimpi Mud Volcano Field (OMVF) is located in the central-northern Mediterranean Ridge (MR) and is comprised of several mud structures. The MR is relatively a deep marine (~1700-2000m) area in the eastern Mediterranean Sea which is uplifted by compressional strengths, triggered by the coalition and subduction of the African plate below the Aegean plate. The MR represents the accretionary wedge of this subduction zone and the marine region offshore southern Crete is considered a forearc basin. The mud volcanism is probably related to backthrusting along the northern border of the accretionary wedge near the backstop region (Robertson et al, 1998). The sediments extruded from the MVs originate from sub-salt (pre-Messinian) layers and consists of a mixture of various lithology and consolidation clasts, supported by an unconsolidated sandy mud (silt and clay at various analogies). In terms of petrology, most of the clasts within the mud breccias are thought to be derived from the North African passive margin, except of various ophiolite-related lithoclasts that are probably derived from higher thrust sheets of Crete (Robertson et al, 1998). The study of the mud breccia provides the only chance to study the deep-seated sub-salt layers in the region, due to the lack of deep wells.

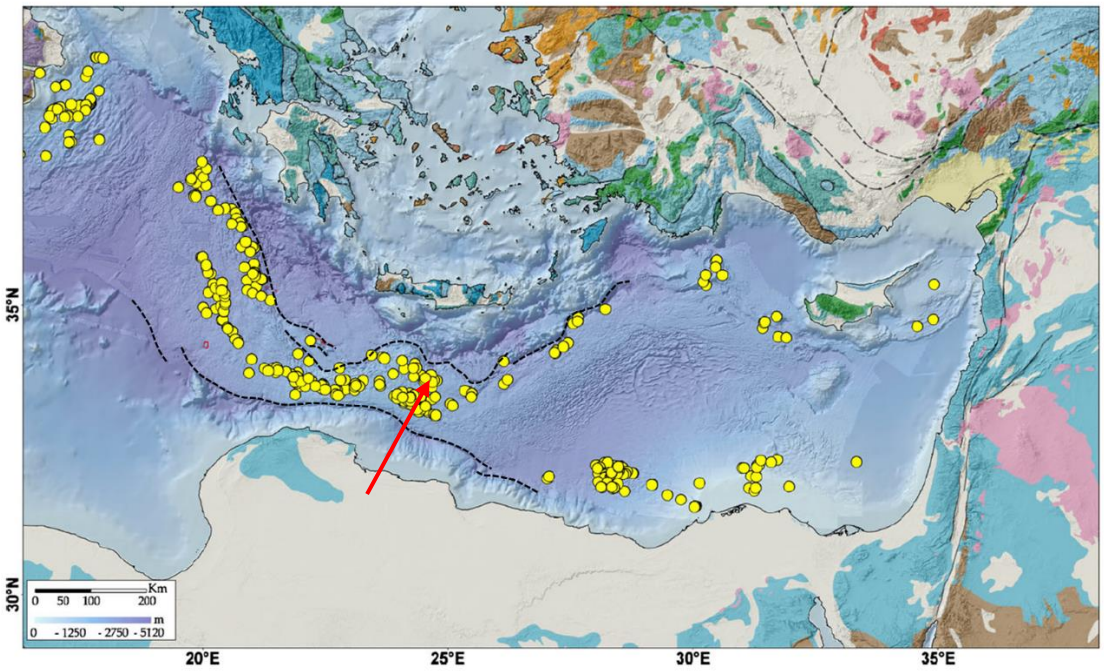

Figure 1. Spatial distribution of mud volcanoes in the eastern Mediterranean Sea. Dashed line shown the northern and southern border of the Mediterranean Ridge (MR) and the red arrow shows the approximate position of the Olimpi Mud Volcano Field (OMVF). Modified from: Mascle et al., 2014

Geotectonic setting

The OMVF is formed in the MR, which represents the accretionary wedge in the geotectonic environment of the subduction of the African below the Aegean plate. The area is characterized by the development of major reverse and thrust faults which affects the deposited sediments. The compressional tectonic regime developed in the MR consists of the latest event of the cyclic tectonometamorphic process of alternate compression and extension that took place during the migration of the Hellenic orogenic belt toward the most external (southern) units (Fassoulas et al, 1994).

During Oligocene-early Miocene, Crete (and Peloponnese) were under N-S compressional regime, developing thick continental crust due to the stacking of the Cretan nappe piles (Plattenkalk, Phyllites/Quartzites, Gavrovo, Pindos, etc.).

The lower part of the nappes (Plattenkalk and Phyllites/Quartzites series) have undergone a HP/LT metamorphism at late Oligocene - early Miocene (Fassoulas et al, 1994) due to burial and overburden pressure from the upper nappes. More recent studies from Samaria gorge (Crete) has shown that metamorphism of Plattenkalk unit took place during early Late Miocene and was not very intense in terms of temperature, as it didn't exceed 300^{o}C (Manoutsoglou et al., 2003).

The upper nappes (Gavrovo, Pindos) remain unmetamorphosed until recent, although at the base of Gavrovo nappe, weakly metamorphosed Permo-Triassic clastic sediments intercalated with carbonates and volcanics (Ravdoucha Beds) (Kilias et al., 1993).

Afterwards, during Miocene-Pliocene the lithospheric plate convergence zone (and consequent compression) migrated southwards, in the Mediterranean region offshore southern Crete and offshore southern Peloponnese (Mountrakis, 2002). As a result, compression in the Mediterranean, led to the onset of the Mediterranean Ridge (MR) development. At the same time, Crete and Peloponnese which were experiencing compressional strengths, are now under N-S extensional tectonic regime. In the Miocene-early Pliocene, crustal extension in Crete caused the uplift of the lower nappes (Kilias et al., 1993) and sedimentary basins were developed onshore and offshore (backstop area) Crete and Peloponnese. Tectonic windows are formed as a result of normal and detachment faults action and exhumation of the -during Oligocene- HP/LT metamorphosed series took place. Characteristic tectonic windows are Taygetos and Psiloritis Mountains in Peloponnese and Crete respectively (Mountrakis, 2002). Miocene syn-sedimentary basins, can be found today in Crete, outcropping in Messara, Potamida, Faneromeni, Gavdos island, etc.

The ongoing (since Miocene-Pliocene) compressional regime in the MR is considered to have triggered the mud volcanoes development during early Pleistocene age (first eruption at 1.25-1.5 Ma for Napoli MV and 1.75 Ma for Milano MV, from: Emeis et al., 1996).

Previous studies

ODP site 970 & 971 (leg 160)

During ODP leg 160, four holes were drilled at the flank and the crest of the Napoli and Milano mud structures (Sites 970 and 971 respectively). Results indicates that the two mud structures do not share any major differences.

Sediments in Napoli MV structure (Site 971) are comprised of the typical mud breccia deposits. Clastic intercalations are included in mud breccia deposits, indicating paucity of eruptive activity and deposition of pelagic sediments and/or high-density turbidites. The matrix of the debris flows (mud breccia) is a complicated mixture of silt, sand and coarser material including nannofossils, foraminifers, clay, quartz, and rock fragments. Clasts are angular to rounded and comprise mainly of claystone, sandstone or limestone. All clasts are considered of Burdigalian-Langhian age. In addition, cores from the crestal areas of Milano MV include layers of ''mousselike'' sediments, indicating the presence of gas seeps. the 'mousselike'' sediments also is an evidence of gas hydrates occurrence. The holes drilled in the flank of Napoli MV show a strong

increase in salinity downhole, which is can be explained by the diffusion and upward migration of brines from underlying, possibly Messinian evaporitic layers. In addition, methane is recorded in the crestal sites.

Sediments in Milano MV (Site 971) structure are also comprised of typical mud breccia deposits. Nannofossil assemblages in the matrix include Pleistocene, middle Miocene, Oligocene, and Eocene species, although clasts are considered of Miocene age, with reworked microfossils of Oligocene, Eocene, and Cretaceous. In addition, hydrocarbon gases were found actively venting from the mud volcano, but gas hydrates were not observed. Except from methane, higher hydrocarbons are present, indicating a partly thermogenic origin. Very high alkalinity was detected in sediments probably reflecting microbial consumption of methane, which is also indicated by a local downward decrease in sulfate.

Eruptive assessment of the MVs – origin of mud breccia

Panagiotopoulos et al. (2020) examined five sediment cores recovered from the Gelendzhik, Moscow, Milano, Leipzig and the newly discovered Heraklion MVs of the Olimpi mud volcano field (OMVF) during LEVECO cruise (2016). An attempt to assess the recent eruptive activity in the OMVF and identify the mud breccia's origin and mobilization depth was made. Sedimentary facies were determined according to the grain size analysis and biomarkers analysis (concentration of n-alkanes, hopanes and steranes) was performed for each facies. Considering the MV's eruptive activity, Milano, Leipzig and Heraklion structures appear to have been ''recently'' active, while Moscow seem to have remained in dormancy for at least one century. In addition, based on hydrocarbon biomarker analysis, the sediments appear to be thermally immature for oil generation, as they are considered to be subjected to temperatures of 35 to 60^{o}C, suggesting a burial depth shallower than 2 km bsf (based on the local geothermal gradient - 30–35 ^{o}C/km). The organic matter of all the MVs is considered of mainly terrestrial higher plants origin (as indicated by the nC29 and nC31 alkane peaks and CPI values), while a minor algal contribution is also recorded. Regarding the age of the extruded sediments a Messinian age was proposed for the very soft - soft mudflows, while an Early-Middle Miocene age was proposed for the firm - very stiff mudflows

Hydrocarbon gases

Methane and other higher hydrocarbons have been recorded in samples from the mud breccia of Napoli and Milano mud structures (Emeis et al., 1996). Gases were composed of methane with light carbon isotopic signature and high abundance of C_{2+} hydrocarbon gases that suggest an (at least) partly thermogenic origin (Camerlenghi et al., 1992). Due to the fact that bacterial methanogenesis reaches its higher limit at temperature of ~80^{o}C (Peters et al., 2005), the minimum depth at which the thermogenic components of the gases are produced should be 2.2-2.6 km with respect to the observed geothermal gradient of 30-35 ^{o}C/km within the Olimpi mud volcano field (Camerlenghi et al., 1995).

Formation water and temperature reconstruction

Pore waters from the Milano mud structure indicate the occurrence of gas hydrates at relatively shallow depths in the sediment (De Lange & Brumsack, 1998). De Lange & Brumsack (1998) assumed that, a massive cap of gas hydrates acts as a cap, preventing the assumed natural gas from escaping.

Experience with formation water temperature reconstruction from mud volcanoes (Barbados accretionary wedge) by Martin et al. (1996), has shown that the most consistent and reasonable temperature reconstructions are achieved with cation geothermometers involving K, Na, and Mg. Haese et al. (2006) calculated the formation water temperatures of seeping fluids from empirical geothermometers in order to predict the depth of fluid origin and geochemical reactions in the deeper subsurface. Multiple fluid sources were determined and formation water temperatures of 55 to 80^{o}C were derived for expelled fluids of the Milano mud volcano (Olimpi area). Given the calculated formation water temperature for Milano seep fluids of 55–80 ^{o}C and a reconstructed maximum mud burial temperature roughly estimated at 51 ^{o}C (vitrinite reflectance data; Kopf et al., 2000), the depths of fluids and mud appear to be similar.

On Milano mud volcano, fluids with enriched and depleted salinities relative to sea water are found only few hundred meters apart from each other. This implies that multiple sources of fluids and respectively different conduits of fluid transport may feed cold seeps of one mud volcano. The Cl^- data span a wide range of concentrations, from extremely depleted with compared to seawater (60 mM) at the crest of Milano dome (site 970) to strongly enriched (up to 5.4 M) at Napoli dome (site 971). The process characterizing the isotopic composition of the fluid is found to be clay mineral dehydration. Chloride enrichment is thought to take place due to dissolving Messinian evaporites, while the extreme Cl^- depletion is caused due to clay mineral dehydration (mainly smectite dehydration to illite) at a depth range of 3.5-7 km and a temperature range of about 120-165^{o}C (Dählmann & de Lange, 2003).

Evidence on organic maturity of the mud breccia

Schulz et al (1997), was the first to evaluate the thermal maturity of the mud breccia matrix extruded from Napoli mud volcano through organic petrography. Based on vitrinite reflectance and fluorescence data, they determined three distinct generations of organoclasts:

- Generation I, with Vr~0.4%, which represents the most abundant organic particles and is interpreted as organic matter from recent in situ (hemipelagic) sedimentation, deposited during the emplacement of the mud breccia.
- Generation II, with Vr=0.65-0.90%, indicating oil window maturities and kerogen of type III. In addition, a mostly terrigenous source material is assumed and possibly a lacustrine or riverine environment.
- Generation III, with Vr>1.4% indicating oxidized and post mature organic matter. Particles of this category are considered reworked.

Kopf et al. (2000), produced thermal maturity data of Milano mud volcano, studying both clasts and mud matrix through vitrinite reflectance study. Their results resembled previous studies (Schulz et al, 1997), as four maturity populations were defined:

- Maximum I: Vr=0.3-0.45%
- Maximum IIa and IIb: Vr= 0.55-0.74% and 0.75-0.95% (reworked)
- Maximum III: Vr>2% (reworked)

Kopf et al. (2000) considered that ‘’Maximum I’’ (Vr=0.3-0.45%) is indicative of the true burial depth of the sediments and its consequent thermal alteration, based on the fact that thermal maturation is an irreversible process and thus the minimum vitrinite reflectance record is indicative of the true burial event. Vitrinite assemblages of higher reflectivity values are considered reworked.

On the contrary Schulz et al. (1997) considered the ‘’Generation II’’ (Vr=0.65-0.90%) indicative of the mud’s burial depth and thermal maturation. Lower reflectivity values ‘’Generation I’’, (Vr~0.4%) were assumed to represent organic matter from Early to Middle Pleistocene (hemipelagic) sedimentation that undergone an early diagenesis, as it deposited and mixed with the extruded mud breccia.

An important difference between the above studies is the fact that the Early to Middle Pleistocene pelagic sediments (0~45m mbsf) near the Milano dome, lacks the ‘’Maximum I’’ maturity population (Kopf et al., 2000), which supports the assumption that the ‘’Maximum I’’ maturity population indicates the stratigraphic origin of the mud.

A second difference is that in Kopf et al. (2000) some clasts lack the (assumed reworked) ‘’Maximum II (a and b)’’ organoclasts, indicating different depositional environment. Robertson & Kopf (1998a) had previously considered a southern origin (African passive margin) of these clasts with respect to the petrographic analyses conducted, while the rest of the clasts were thought to be derived from the Cretan tectonic nappes.

Materials and methods

The five (5) sediment cores studied in this project, were recovered onboard R/V Aegaeo of the Hellenic Centre for Marine Research (HCMR) during the LEVECO oceanographic expedition (2016). Coring positions correspond to the crests of the Gelendzhik (Lev1GC), Heraklion (Lev3GC), Moscow (Lev5GC), Milano (Lev7GC) and Leipzig (Lev9GC) structures. According to Panagiotopoulos et al. (2020), the sampling locations (Fig. 1a) being selected according to the intensity of the backscatter signal obtained from the swath bathymetry data (Fig. 1b). The sampling process was performed using a gravity corer (Benthos) with a 3m-long core barrel. Due to the highly incohesive nature of the majority of the mud breccia deposits, the recovery length of the retrieved cores was generally incomplete (70–132 cm) (Panagiotopoulos et al., 2020).

In the laboratory, samples were taken from the cores and clasts were carefully divided from the mud matrix. In total, forty-two (42) samples were produced and described regarding their color, lithology and consolidation.

Thereafter, the samples were divided in two almost equal proportions and

- the first half was completely homogenized using a mortar and pestle and proportion of at least 100 mg per sample, were subjected to Rock Eval pyrolysis.
- the second half was used to produce smear slides for microscopical study of the calcareous nannoplankton content, according to Marsaglia et al (2014).

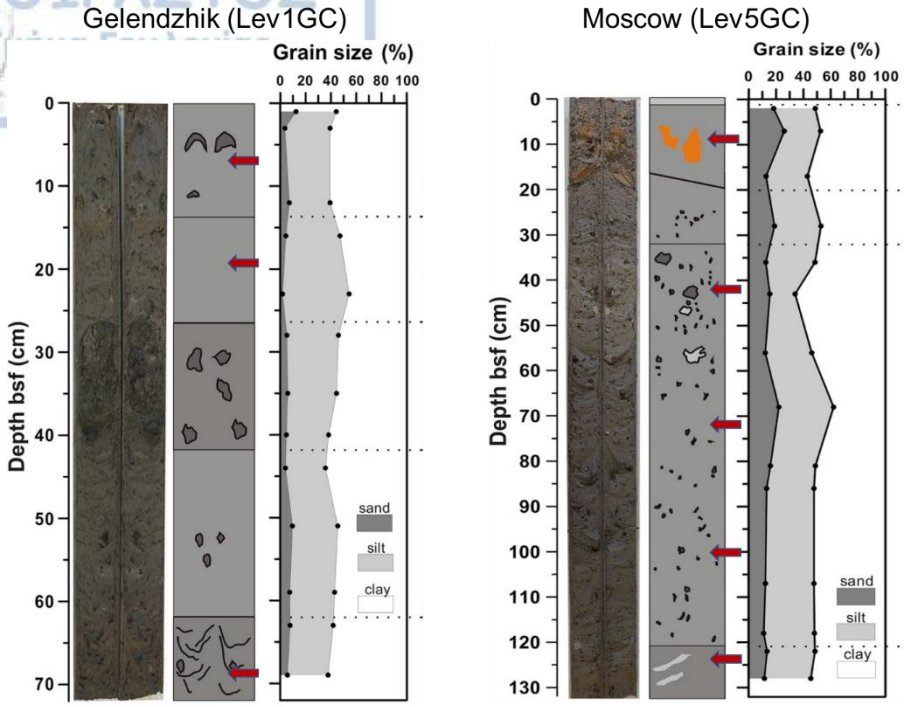

Figure 2. Picture of cores recovered from Gelendzhik and Moscow MVs, showing the core length, distinct sedimentary facies and high-resolution grain size analysis through the core. Red arrows show the sampling location intervals. Modified from Panagiotopoulos et al. (2020).

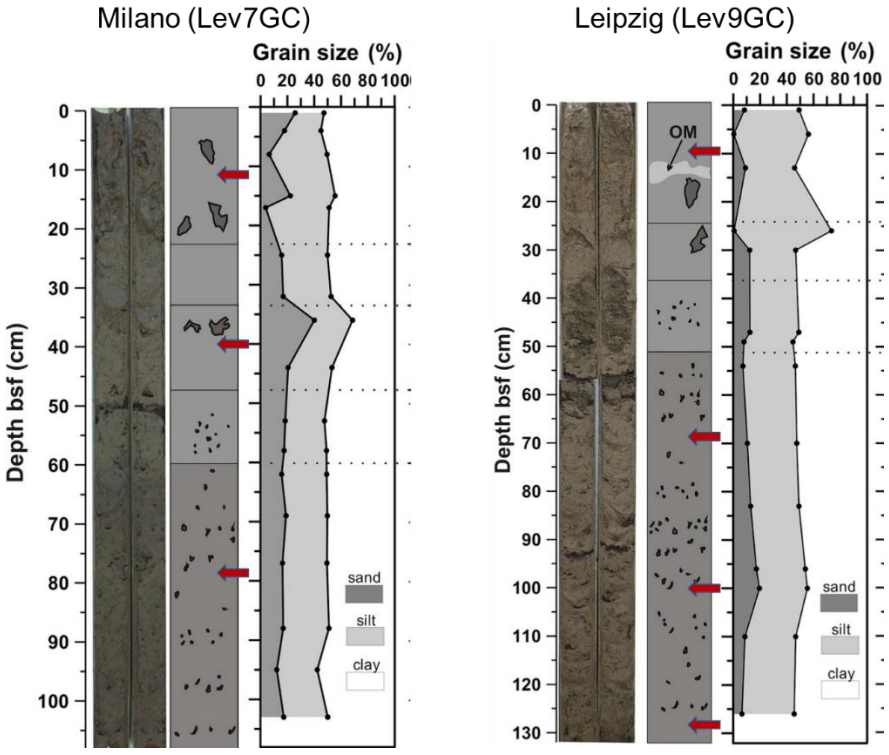

Figure 3. Picture of cores recovered from Milano and Leipzig MVs, showing the core length, distinct sedimentary facies and high-resolution grain size analysis through the core. Red arrows show the sampling location intervals. Modified from Panagiotopoulos et al. (2020).

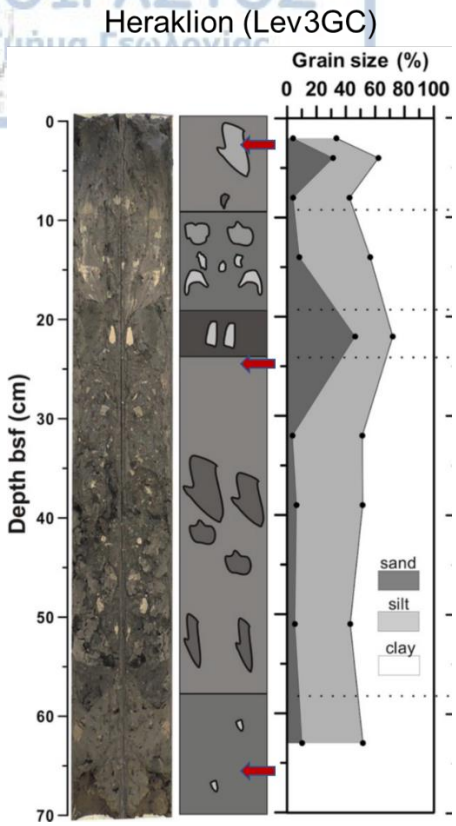

Figure 4. Picture of core recovered from the newly discovered Heraklion MVs, showing the core length, distinct sedimentary facies and high-resolution grain size analysis through the core. Red arrows show the sampling location intervals. Modified from Panagiotopoulos et al. (2020).

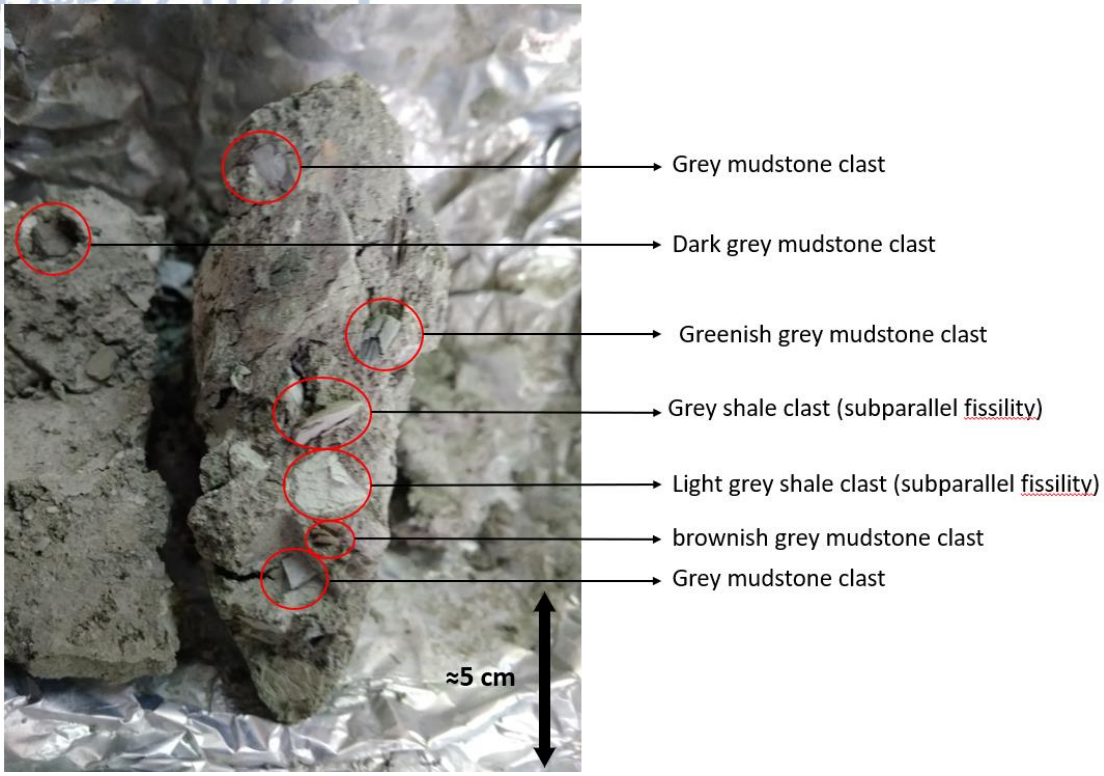

Figure 5. Typical core interval. Similar image is observed through all the LEVECO cores.

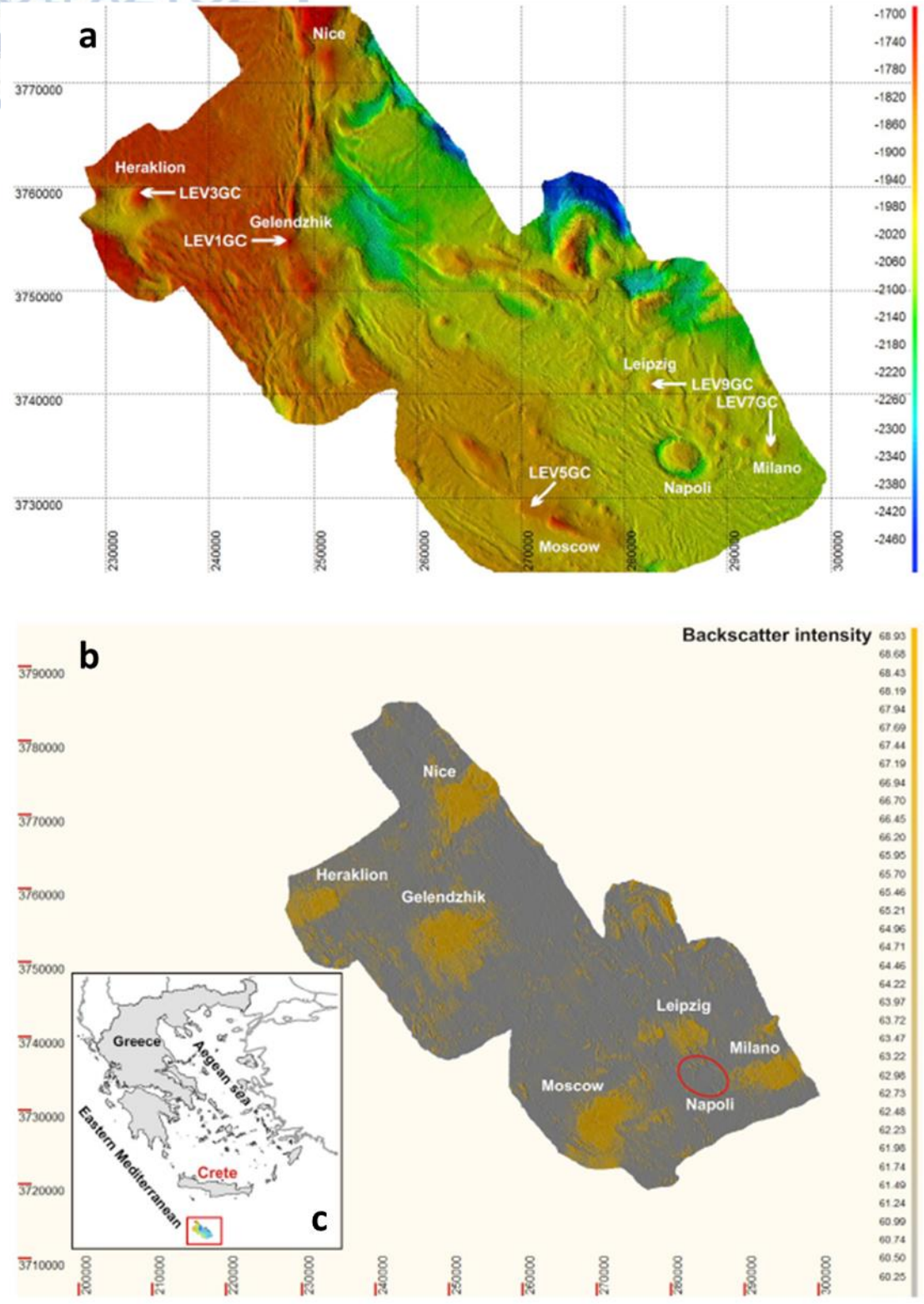

Figure 6. a: Bathymetric digital terrain model of the Olimpi mud volcano field (grid interval: 50 m; ellipsoid: WGS84; projection: UTM35N; reference datum: mean sea level) and sediment coring locations (the core labels appear in white color). b: Seabed reflectivity in the Olimpi mud volcano field (grid interval of 50 m); the yellow-colored patches represent strong backscatter signal. c: Location of the Olimpi mud volcano field (inset map). Modified from Panagiotopoulos et al. (2020).

Micropaleontology – Biostratigraphy

Extensive semiquantitative analysis was conducted in up to ~300 fields of view per slide in longitudinal traverses randomly distributed (3 traverses; 100 fields of view per traverse). The traverses were representing both low- and high-density material content and in any case, counting of at least 150 specimens have been achieved, in an effort to make accurate nannofossil determinations and trace even the rarest species. The microscopical analysis was conducted using a Leica DMLSP optical polarizing light microscope at 1250 ×, in the Department of Historical Geology — Palaeontology, Faculty of Geology and Geoenvironment, University of Athens.

As proposed by Triantaphyllou (2013) the nannofossil data are presented using the standard biozonal scheme (Martini, 1971), as this has been incorporated in the magnetobiochronologic framework (Berggren et al., 1995) and revised concerning the numerical ages (Lourens et al., 2004, Luterbacher et al., 2004).

Semiquantitative abundances of the taxa encountered were recorded as follows:

Abundant	≥ 1 specimen / 1 fields of view
Common	≥ 1 specimen / 10 fields of view
Few	1 specimen / 10–50 fields of view
Rare	1 specimen / > 50 fields of view

Table 1. Semiquantitative characterization of the recorded specimen abundances.

Sample preparation imperfections due to the nature of the samples could result in reworking of nannofossil species and organic material. Specifically, it is possible that several matrix samples contained minor clasts (e.g. coarse sand sized) of different stratigraphic origin, which are difficult to distinguish. Grinding and homogenizing the matrix and minor clasts could lead to a sample of different organic matter types of and different nannofossil assemblages. In addition, clasts which contain organic matter and nannofossils of different stratigraphic origin could be explained by the presence of possible residual matrix proportion that hasn't been scraped off sufficiently from the clasts' surface during sample preparation and as a result been homogenized along with the clast's body.

Organic geochemistry – Rock Eval pyrolysis

The samples, after being pulverized and dried at 40ºC, were subjected to Rock-Eval pyrolysis, following the guidelines of Espitalié et al. (1977). Each sample was heated in an inert He atmosphere for 2 minutes at 300ºC and then pyrolyzed stepwise with increasing temperature at 600ºC with a heating rate of 25ºC/min. The measured parameters of each pyrolysis run consist of three peaks (S1, S2, and S3) and a maximum temperature value (Tmax).

- S1: equals to the quantity of free hydrocarbons contained in the sample. Measured in mg HC/g rock.
- S2: equals the quantity of hydrocarbons produced by thermal conversion of kerogen contained in the sample. Measured in mg HC/g rock.

- S3: equals the quantity of organic CO_2 produced during pyrolysis from the organic matter in the sample. S3 is indicative of the oxygen content in kerogen. Meaured in mg CO_2/g rock.
- Tmax: equals the temperature corresponding to the maximum generation of hydrocarbons from kerogen.

Additionally, during Rock-Eval pyrolysis, the total organic carbon (TOC) and mineral carbon (MINC) content of the samples is calculated from the S1, S2 and S4 peaks. The S4 peak corresponds to the CO_2 generated from the oxidation in air at 600°C of the residual carbon (after pyrolysis). The S4 peak record is not included in the results.

Lastly, Hydrogen (HI) and Oxygen (OI) indices were calculated, using the previous parameters.

- HI is defined as (100 x S2)/TOC. The HI is indicative of the amount of hydrogen included in the kerogen.
- OI is defined as (100 x S3)/TOC. The OI is indicative of the amount of oxygen included in the kerogen.

The Rock-Eval pyrolysis was conducted in a Rock-Eval VI (Delsi Inc.) in the Institute of Petroleum Research-FORTH, University Campus, 73100 Chania, Greece.

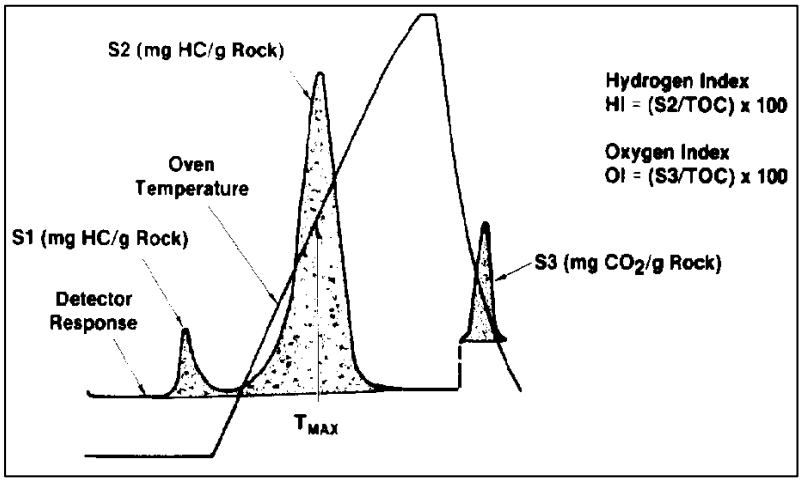

Figure 7. Schematic image of pyrogram showing evolution of organic compounds and recording of S1, S2 and S3 peaks. From Peters et al., 1985

Results and discussion

Calcareous nannoplankton Micropaleontology – Biostratigraphy

Mudstone/shale clasts samples

Older studies indicate that the mudstone clasts from the Prometheus 2/Olimpi MV are of Burdigalian-Langhian age, containing reworked Oligocene, Eocene and Cretaceous nannofossils (Emeis et al., 1996a and 1996b; Silva et al., 1996; Staffini et al., 1993; Silva et al., 1996).

In this study, Burdigalian-Langhian mudstone/shale clasts are very common, containing nannofossil assemblages characterized by the coexistence of

- *Sphenolithus heteromorphus* (NN4-NN5) and *Helicosphaera ampliaperta* (NN2-NN4) attributed to NN4 biozone, found in four (4) mudstone/carbonate mudstone samples – Heraklion, Moscow and Leipzig MVs
- *Sphenolithus heteromorphus* (NN4-NN5) and *Coccolithus miopelagicus* (NN5-NN8 biozone) attributed to NN5 biozone, found in two (2) carbonate mudstone clast samples – Moscow and Leipzig MVs

Along with the above age diagnostic species, a typical Miocene long-range species such as *Reticulofenestra pseudoumbilicus, Reticulofenestra pseudoumbilicus* <5μm, *Helicosphaera carteri, Umbilicosphaera jafari* and other Paleogene-Neogene long range species like *Coccolithus pelagicus, Sphenolithus moriformis, Cyclicargolithus floridanus, Discoaster deflandrei, Coronocyclus mesostenos, Helicosphaera intermedia, Coccolithus miopelagicus, Reticulofenestra perplexa* and others.

In addition, for the first time in the Prometheus 2/Olimpi MV field, Oligocene mudstone/shale clasts were found. Based on calcareous nannofossil assemblage study, three (3) clasts derived from Moscow (1 shale and 2 mudstone clasts) MV, were placed in NP23-NP24 biozones. In detail:

- Sample LEV5bGC 40-42 clast 1, contains a typical NP24 biozone assemblage, characterized by the occurrence of *Sphenolithus distentus* (NP23-NP24), *Sphenolithus predistentus* (NP16-NP24) and *Sphenolithus ciperoensis* (NP24-NP25) along with other Paleogene-Neogene long-range species (*Coccolithus pelagicus, Cyclicargolithus floridanus, Discoaster deflandrei, Sphenolithus moriformis, Coronocyclus mesostenos Zygrhablithus bijugatus*, etc.).
- Sample LEV5bGC 10-12 clast 1, is characterized by the occurrence of *Sphenolithus distentus* (NP23-NP24), *Sphenolithus predistentus* (NP16-NP24) and *Sphenolithus peartiae* (NP23-NP24) and is placed in NP23/NP24 biozone. Along with the typical Paleogene-Neogene long-range species, also some species of Miocene age were recorded (*Coccolithus miopelagicus, Discoaster discissus, Discoaster durioi, Discoaster exilis, Gephyrocapsa < 3 μm, Helicosphaera carteri, Sphenolithus abies*). This limited Miocene assemblage is thought to be produced during sample preparation procedure. (see ''other reworking parameters'').
- Sample LEV5bGC 100-102 clast 1, is characterized by the occurrence of *Sphenolithus distentus* (NP23-NP24) and *Sphenolithus peartiae* (NP23-NP24) and is placed in NP23/NP24 biozone. Along with the typical Paleogene-Neogene long-range species (*Coccolithus formosus, Cyclicargolithus floridanus, Discoaster deflandrei*, etc.), also some species of Miocene age were recorded (*Coccolithus miopelagicus, Discoaster kugleri, Reticulofenestra pseudoumbilicus, Umbilicosphaera jafari*). This limited Miocene assemblage is thought to be produced during sample preparation procedure. (see ''other reworking parameters'').

It is worth mentioning that the above newly found Oligocene nannofossil assemblages, resembles very much the typical (age equivalent) Gavrovo flysch assemblage from southeastern Aitoloakarnania section (Triantaphyllou, 2013) with respect to its microscopical image observations.

Lastly, the youngest age for the clasts contained in the mud breccia is determined as Serravallian (NN6 and NN7 biozones). Based on calcareous nannofossil assemblage study, four (4) mudstone clasts samples (Gelendzhik and Moscow MVs) were placed

in NN7 biozone and six (6) mudstone/shale clasts samples (Gelendzhik, Milano and Leipzig MVs) were placed in NN6 biozone. In detail:

- NN7 biozone assemblages were characterized by the occurrence *of Discoaster kugleri* and the absence or very small abundance of *Cyclicargolithus floridanus*, last occurrence of which takes place during NN6.
- NN6 biozone assemblages were characterized by the occurrence of *Reticulofenestra pseudoumbilicus, Calcidiscus macintyrei* and the presence (small abundance) of *Cyclicargolithus floridanus*, last occurrence of which takes place during NN6.

The very low recorded numbers of *Cyclicargolithus floridanus* in some samples may show an age very close to its last occurrence or indicate reworking of these species from older sediments.

Along with the above typical NN6 and NN7 assemblages, other long-range species of Paleogene-Neogene age were recorded in the assemblages (*Helicosphaera carteri, Cyclicargolithus floridanus, Discoaster deflandrei, Sphenolithus moriformis* and other).

LEV1cGC 4-6 clast 1 shows some special characteristics regarding both its microscopical image and geochemical values. Microscopically, it is characterized by great abundance of both calcareous and siliceous microfossils, which indicates great primary production by the time of the sediment deposition (NN7 biozone – upper Serravallian age). In addition, Rock Eval pyrolysis shows high TOC value (2.02 wt. %) along with high HI and relatively low OI (438 and 91 respectively), which indicates low oxygen availability (anoxic/hypoxic conditions) during deposition and preservation of organic matter. It is possible the sea bottom anoxic/hypoxic condition were triggered by the great abundance of (micro)fauna in the euphotic zone and the consequent great need of oxygen. The continuous consuming of oxygen in the euphotic zone restricted or cut the oxygen transportation to the deep-sea layers causing anoxic/hypoxic conditions and elimination of aerobic sea bottom life. The organic matter precipitated to the seafloor from the euphotic zone or from river input, was preserved due to the absence of aerobic bacteria which could consume the organic matter. Taking into account the above clues, sample LEV1cGC 4-6 clast 1 can be characterized as sapropel.

The oldest known sapropels in the Mediterranean sedimentary sequences are considered of Langhian age (~15.4 Ma) and can be found onshore Northern Cyprus in a section of predominantly marl successions (Taylforth et al., 2014).

DSDP leg 42A site 375 (offshore western Cyprus), managed to drill sapropels also as old as Langhian with the oldest layer attributed to the NN5 biozone (Kidd et al., 1978). In the same project a distinct sapropel was recorded that resembles the characteristics of sample LEV1cGC 4-6 clast 1, regarding its age (NN7 biozone) and organic content (2 wt.%). Considering the fact that recent sapropels (Plio-Pleistocene and Holocene layers) are well studied and correlated across the Mediterranean, it is proposed that the sapropel of LEV1cGC 4-6 clast 1 can be correlated with the one attributed to NN7 biozone during DSDP leg 42A site 375 offshore western Cyprus.

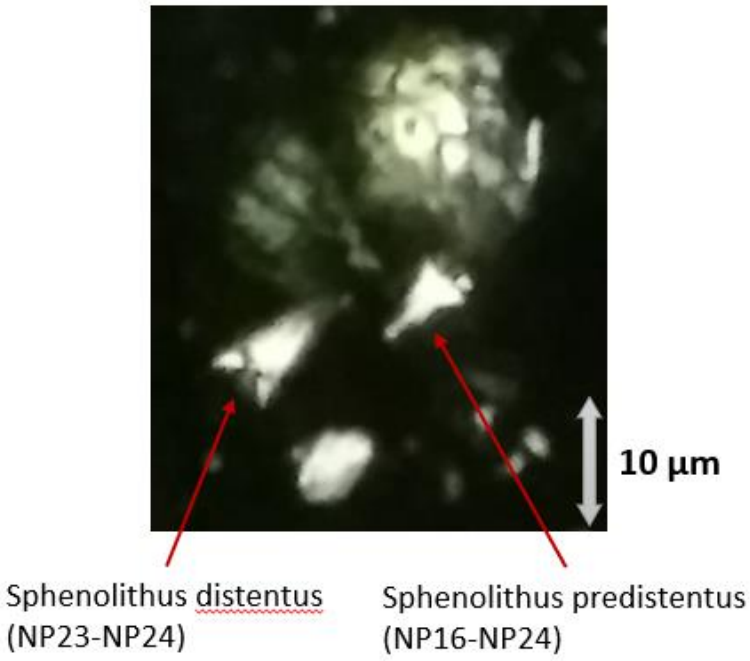

Figure 8. Sphenolithus distentus, Sphenolithus predistentus (pictured above), along with Sphenolithus ciperoensis defines the NP24 biozone. Picture from LEV 5b GC 40-42 clast 1 sample.

Matrix samples

Concerning the matrix samples, a mixed Miocene-Oligocene assemblage is indicated for all the samples reflecting a multi-source feeding of the MVs and heavy sediment mixing. However, one matrix sample (LEV3cGC 2-5 matrix) appeared to be barren of nannofossils, showing the high degree of heterogeneity along the mud breccia body. It is proposed that the mixing of the sediments is caused due to (1) the initial mixing of

mud from different sources when they enter the MVs feeder conduit and (2) a further mixing of the sediments during expulsion to the sea floor.

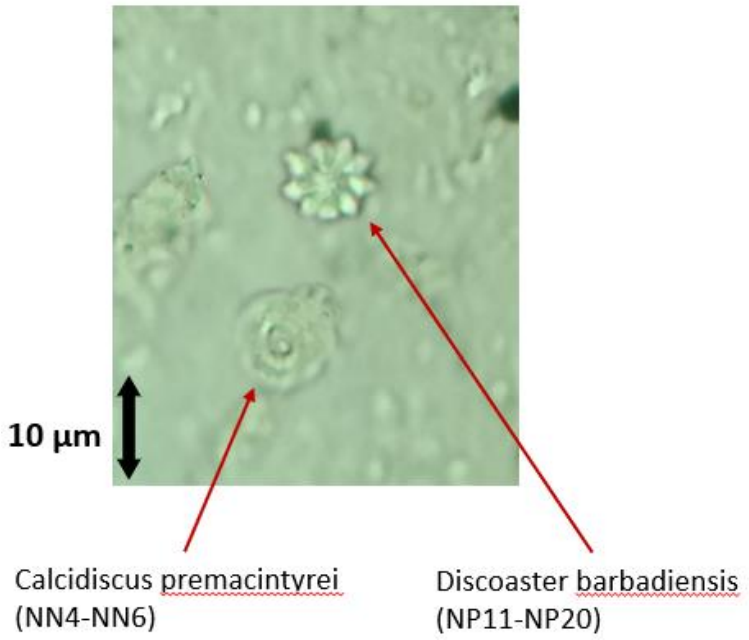

Figure 9. Calcidiscus premacintyrei and Discoaster barbadiensis. A Miocene and an Eocene species found at the same microscopical image is indicative of the heavy reworking. Similar microscopical image is observed in all matrix samples. Picture from LEV 5b GC 10-12 matrix sample.

Significance of reworked species

Almost every sample contains few (~10%) reworked nannofossils of Miocene Oligocene, Eocene and upper and lower Cretaceous age, depending on the sample. However, matrix samples seem to contain mixed assemblages of Miocene and Oligocene species along with older -probably reworked- species of Eocene and Cretaceous age. Mixed assemblages in the mud breccia deposits consist a strong evidence of multi-source feeding of the MV structures. These older (reworked) species provide valuable information concerning the stratigraphy and geological history of the Mediterranean Ridge, which in fact remains a mystery, mainly due to the lack of deep wells in the region.

Specifically, it is observed that:

- The middle Miocene (NN5, NN6, NN7) dated samples contain reworked nannofossils of early-middle Miocene, Oligocene, Eocene and Cretaceous age.
- The early-middle Miocene (NN4) dated samples contain reworked nannofossils of Oligocene, Eocene and Cretaceous age.
- The Oligocene (NP24, NP23-24?) dated samples contain reworked nannofossils of Eocene and Cretaceous age.

A characteristic observation is the absence of Paleocene age species from all samples, a fact that may indicate very thin Paleocene sedimentary layers. In fact, the only clue that would support the existence of Paleocene layers is the presence of *Discoaster*

multiradiatus, the first occurrence of which, takes place in the late Thanetian (latest Paleocene).

The presence of reworked nannofossils in both the Miocene and Oligocene assemblages, indicates a subaerial/subsea exposure, erosion and redeposition of older sediments during that time. Specifically, the recorded assemblages indicate (1) an subaerial/subsea exposure and erosion of Cretaceous and Eocene sequences during Oligocene age (2) an subaerial/subsea exposure and erosion of the Oligocene, Eocene and Cretaceous sequences during early-middle Miocene and (3) an subaerial/subsea exposure and erosion of the early-middle Miocene, Oligocene, Eocene and Cretaceous sequences during middle Miocene.

Taking into account the evidence on reworked species, it is concluded that:

- Sedimentary layers at least as old as lower Cretaceous are present, excluding Paleocene age sediments, due to lack of clues
- Regional uplift and erosion of Eocene and Cretaceous sequences took place during Oligocene
- Regional uplift and erosion of Oligocene, Eocene and Cretaceous sequences took place during early-middle Miocene
- Regional uplift and erosion of early-middle Miocene sequences took place during middle Miocene

It is not clear if the erosion and redeposition of older sediments took place in subaerial or subsea condition – although a combination of both, would seem more realistic. The subaerial exposure and erosion scenario can be supported by the high Oxygen Index (OI) observed in most of the samples - a characteristic of kerogen type III, which indicates high terrestrial input (Killops & Killops, 2013). The subsea erosion (e.g. turbidites) scenario is supported by the fact that the southern Crete region is a highly tectonised area that has experienced both compressional and extensional tectonic regime. In such environments, high inclination slopes are formed, creating favorable conditions for turbidity currents development.

Organic geochemistry – Rock Eval pyrolysis

For the first time, organic geochemical methods (Rock-Eval pyrolysis) was used to determine the organic matter content, quality and thermal maturity of the deep-seated sediments of the Mediterranean Ridge offshore south of Crete.

Organic matter content values for the mudstone/shale clasts fluctuates between 0.11 and 2.02% with an average of 0.57% TOC, while matrix samples show values of 0.25-0.94%, with an average of 0.51% TOC. The two (2) coarse grained clasts show very low TOC values (0.26% for interbedded mudstone/sandstone and 0.03% for the sandstone clast).

Concerning the quality of the organic material, most of the samples (clasts and matrix) show a tight distribution around type III kerogen curve, indicating mainly higher (terrestrial) plant contribution to the organic matter accumulation (Killops & Killops, 2013), which is in accordance with previous studies also indicating a mainly terrestrial origin (Panagiotopoulos et al., 2020). Kerogen type III is typically considered more favorable for gas generation than for oil (Espitalie et al., 1977). Nevertheless, one (1) NN7 (sapropel) sample (mudstone clast – Gelendzhik MV), one (1) undetermined age sample (matrix - Heraklion MV) and one (1) NN4 sample (mudstone clast – Moscow MV), seem to approach kerogen type II curve. Kerogen type II is mainly composed of

marine organic materials (phytoplankton, zooplankton and bacteria) along with allochthonous organic materials (e.g. higher plants) (Killops & Killops, 2013) and is more favorable for oil generation (Espitalie et al., 1977).

In terms of thermal maturation, all the samples are considered immature showing Tmax values lower than the oil window onset (Tmax=435ºC) (Espitalie et al., 1977). However, three (3) NN4 mudstone clasts (Heraklion MV, Moscow and Leipzig MVs) and one (1) mixed Oligocene-Miocene matrix sample (Milano MV) are nearly mature (Tmax=430-434ºC).

Some samples have shown anomalous S2 curves during rock eval pyrolysis performance. These anomalies concern nine (9) clasts (mudstone, shale and sandstone) and two (2) matrix samples and are depicted as wide or bimodal/multiple peaks in S2 curve record, possibly indicating mixture of organic material of different origin and thermal maturity. As a result, Tmax values (which correspond to S2 curve peak) for these samples are considered unreliable and thus were not presented in this study. Most of these clasts show moderate to major reworking concerning the recorded nannofossil assemblage, a fact that supports the organic matter mixing concept. However, two (2) clasts and one (1) matrix sample appear to be almost barren of nannofossils.

The measured mineral carbon content (MINC wt. %) can be used for the calculation of the carbonate content of the samples by using the equation:

$Q_{carbonates}$ = 7.976 * MinC (Jiang et al., 2017)

Where $Q_{carbonates}$ is the carbonate content of the sample and MINC is the mineral carbon content (MINC wt. %) measured from Rock-Eval pyrolysis. According to the results, samples containing $Q_{carbonates}$ > 50% are characterized as ‘’carbonate’’ (e.g. carbonate mudstone).

From a statistical point of view, the critical lower limit for non-reservoir, shale-type (source rock) sediments in oil provinces is considered TOC=0.5% (Tissot & Welte, 2013). Consequently, source rock generative potential is considered poor for TOC values >0.5% and fair for values 0.5-1.0% (Peters, 1986).

Only three (3) of the matrix samples show TOC values greater than 0.5%, while the remaining ten (10) samples are considered poor, with TOC <0.5%. Better results are extracted for the mudstone/shale clasts, which seem to be richer in organic content. Thirteen (13) clasts contain TOC<0.5% and fourteen (14) contain TOC>0.5%.

TOC (wt. %)	Source-Rock Implications
< 0.5%	negligible source capacity
0.5%-1.0%	possibility of slight source capacity
1.0%-2.0%	possibility of modest source capacity
> 2.0%	possibility of good to excellent source capacity

Table 2. Indications of source-rock potential based on TOC values. Redrawn from Waples (2013).

TOC (wt. %)	Quality
< 0.5%	Poor
0.5%-1.0%	Fair
1.0%-2.0%	Good
> 2.0%	Very good

Table 3. Source rock quality based on TOC (wt. %). Modified & redrawn from: Peters (1986).

The results of Rock-Eval pyrolysis are presented at the Appendix for each mud structure along with the age of each sample extracted from the nannoplankton study. Figures 10, 11, 12 and 13, show the interpretation of the results, regarding source rock potential, based on the study of Espitalié et al. (1977) and more recent studies (Espitalié et al., 1985; Hunt, 1995; Jackson et al., 1985).

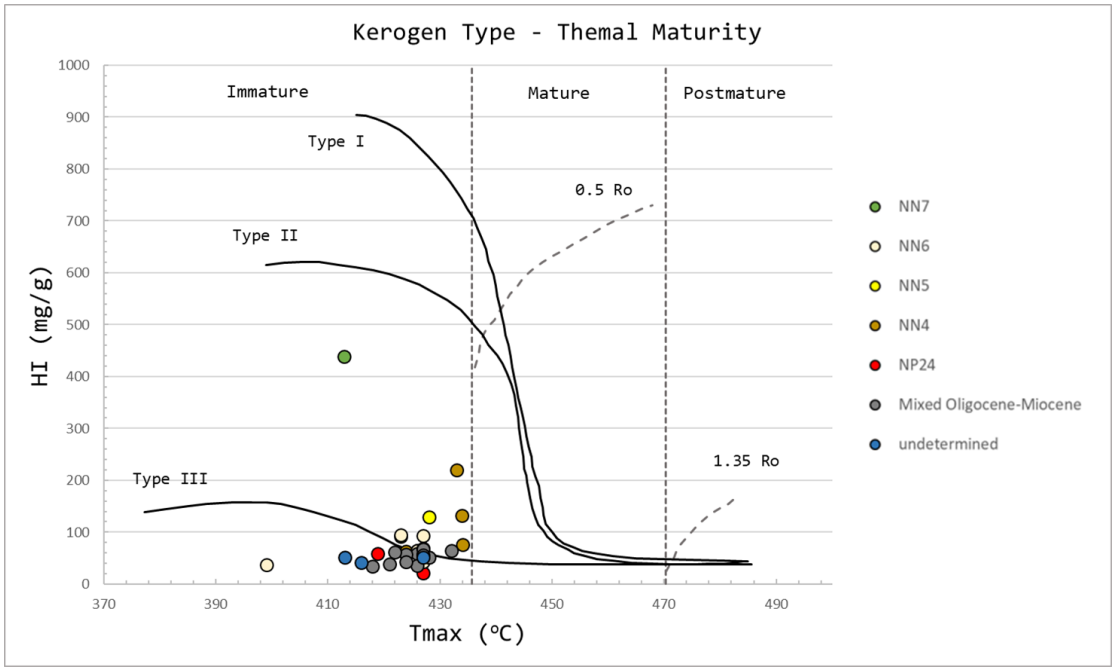

Figure 10. HI versus Tmax plot showing the kerogen type and maturity curves along with the top and base maturity vitrinite reflectance curves.

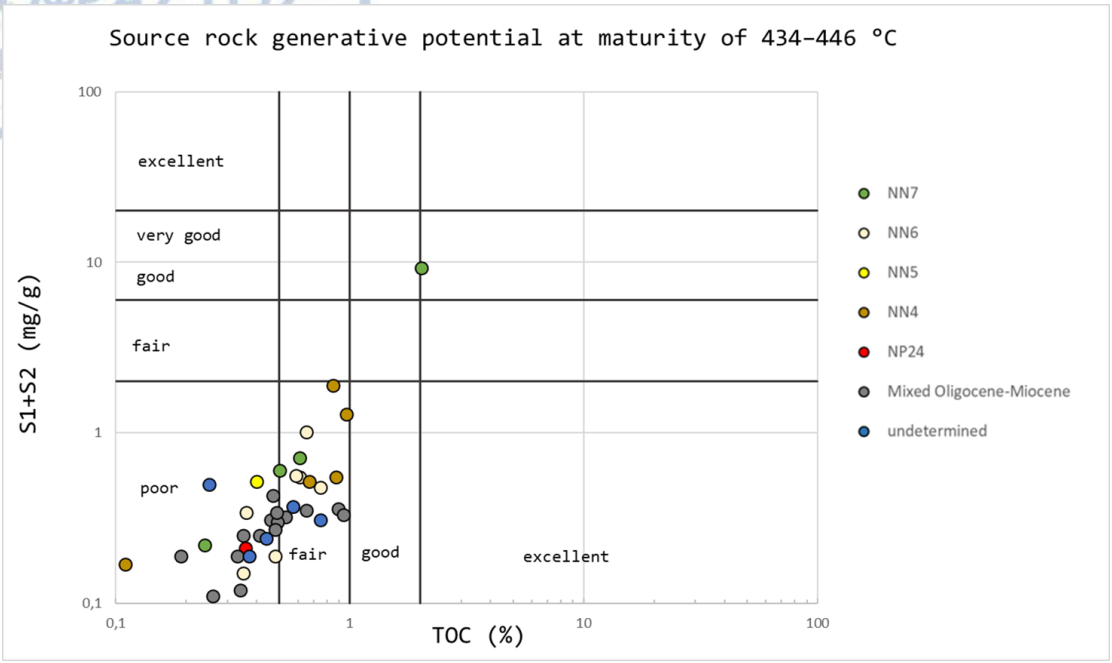

Figure 11. (S1 + S2) versus TOC plot showing the relative quantity of hydrocarbons that the source is capable of producing.

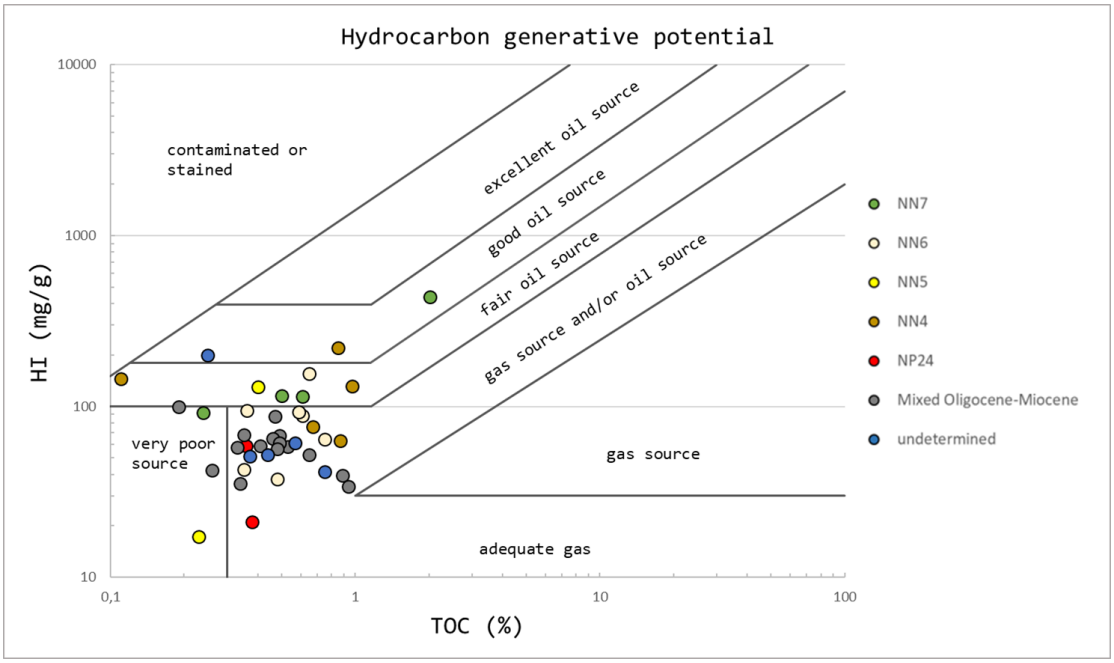

Figure 12. Plot of HI mg/g versus TOC (wt. %) showing the quality of hydrocarbons that the source is capable of producing.

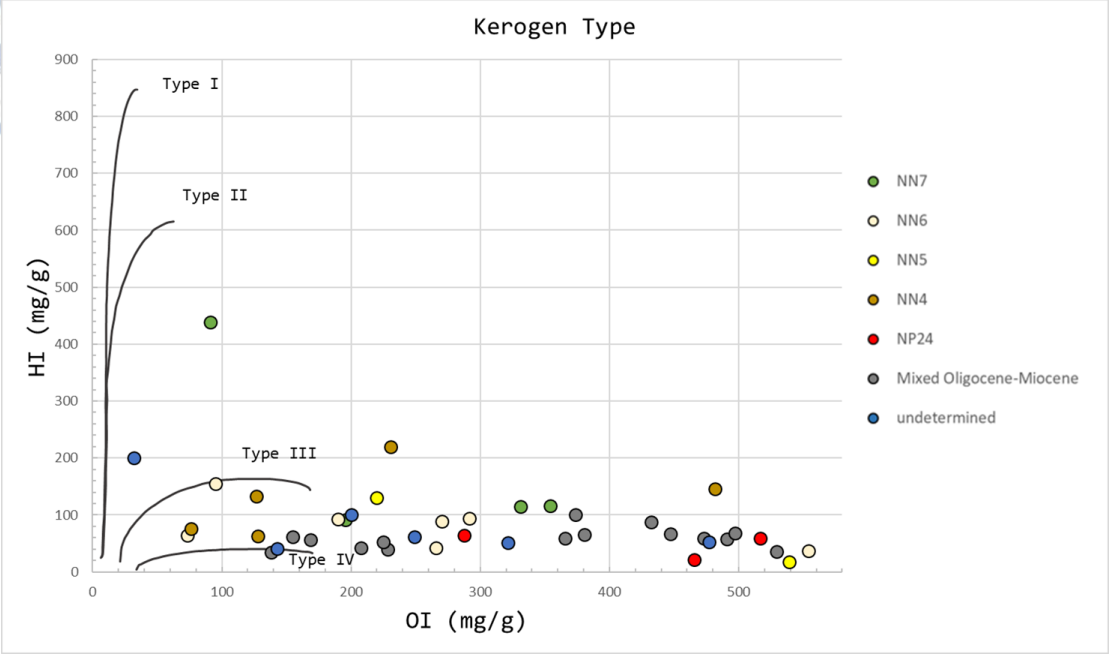

Figure 13. HI versus OI plot showing the kerogen type curves.

Conclusion

This master thesis has attempted to study and produce scientific information concerning the (pre-Messinian) sub-salt sediments in the eastern Mediterranean, south of Crete – an underexplored marine region, with no deep wells. Exact dating of the available sediments (clasts and matrix) was conducted, that for the first time, led to the determination of:

- one (1) NP24 mudstone clast
- two (2) NP23-NP24 mudstone/shale clasts
- four (4) NN7 mudstone clasts

among the NN4, NN5, NN6 dated samples, which were previously determined by previous studies. In addition, one (1) of the NN7 mudstone samples is found to most probably represent a sapropel of the latest Serravallian, with respect to its microscopical image and geochemical characteristics.

Thereafter, the dated sediments were subjected to Rock Eval pyrolysis, in order to determine the sediments' source rock potential. For the first time, the TOC values, Kerogen Type and thermal maturity of sub-salt sediments in the eastern Mediterranean, south of Crete were determined. The results show:

- a tight distribution around kerogen type III curve
- organic rich (TOC>0.5 wt.%) and organic poor layers (TOC<0.5 wt.%)
- immature (Tmax<434) and nearly mature (Tmax 430-434) samples

An exemption is the sapropel sample, which is characterized by kerogen of type II and very high organic content (TOC:2.02 wt.%). In terms of thermal maturity, the sample is considered immature.

This information can be of great value in oil and gas exploration, as it is the first clue of the existence and stratigraphic origin of oil and gas source rocks, in the pre-Messinian (sub-salt) eastern Mediterranean, offshore southern Crete.

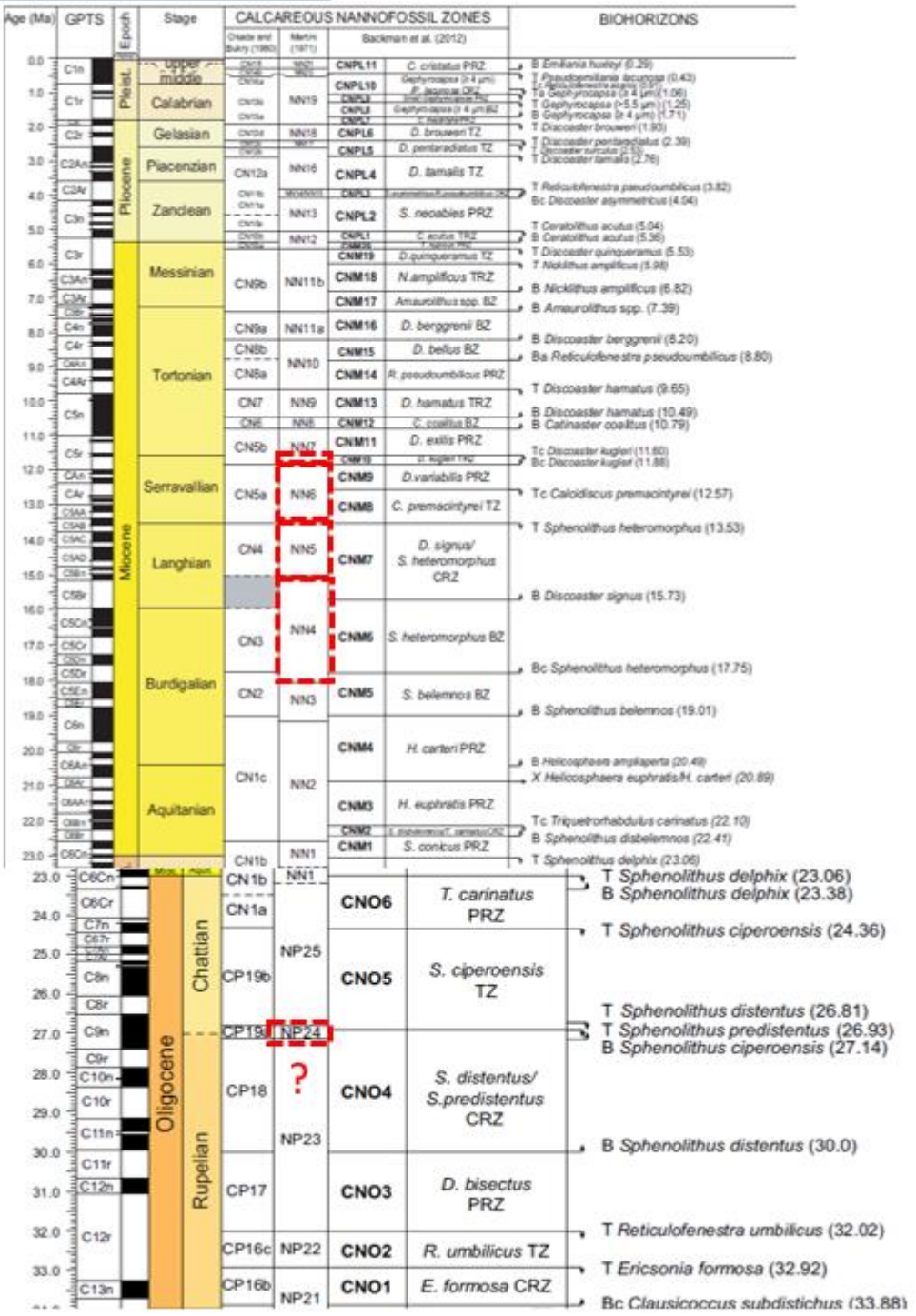

Figure 14. Neogene and Oligocene chronostratigraphic column and biozonation of Backman et al (2012), Martini (1971) and Okada and Bukry (1980) along with some major calcareous nannoplankton events. Red dashed columns represent the biozones determined through this study. Redrawn from: Agnini et al., 2017.

In addition, concerning previous studies on tectonic geology that defined several major tectonic events in Crete and southern Crete region (Fassoulas et al., 1994; Mountrakis,

2002; Angelier et al., 1982; Le Pichon & Angelier, 1979) and combining these studies along with previous (Emeis et al., 1996a and 1996b; Silva et al., 1996; Staffini et al., 1993) and the present sedimentological work, a geological history since Oligocene age, including four (4) major geotectonic events can be well defined and supported.

1. Oligocene compression in Crete-Peloponnese – Mesozoic-Eocene nappe stacking and crust thickening – deposition of Oligocene pelagic/hemipelagic sediments along with Eocene and Cretaceous sediments in future MR.
2. Miocene extension in Crete-Peloponnese (ongoing) – uplift and exhumation of Cretaceous-Eocene-Oligocene sediments – deposition of Miocene pelagic/hemipelagic sediments along with sediments from Oligocene, Eocene and Cretaceous sequences in future MR.
3. Late Miocene – early Pliocene compression south of Crete-Peloponnese (ongoing) – minor (subsea) uplift – MR development onset – deposition of Late Miocene pelagic/hemipelagic sediments along with sediments from early-middle Miocene, Oligocene, Eocene and Cretaceous sequences in MR.
4. Early Pleistocene (Calabrian) further compression in MR (ongoing) – Mud volcanoes development – extrusion of the pre-deposited Miocene-Oligocene sediments with reworked nannofossils of Miocene, Oligocene, Eocene and Cretaceous age. First eruption of Napoli MV at 1.25-1.5 Ma and Milano MV at 1.75 Ma

References

Agnini, C., Monechi, S., & Raffi, I. (2017). Calcareous nannofossil biostratigraphy: historical background and application in Cenozoic chronostratigraphy. Lethaia, 50(3), 447-463.

Aloisi, G., Pierre, C., Rouchy, J. M., Foucher, J. P., & Woodside, J. (2000). Methane-related authigenic carbonates of eastern Mediterranean Sea mud volcanoes and their possible relation to gas hydrate destabilisation. Earth and Planetary Science Letters, 184(1), 321-338.

Angelier, J., Lyberis, N., Le Pichon, X., Barrier, E., & Huchon, P. (1982). The tectonic development of the Hellenic arc and the Sea of Crete: a synthesis. Tectonophysics, 86(1-3), 159-196.

Backman, J., Raffi, I., Rio, D., Fornaciari, E., & Pälike, H. (2012). Biozonation and biochronology of Miocene through Pleistocene calcareous nannofossils from low and middle latitudes. Newsletters on Stratigraphy, 45(3), 221-244.

Camerlenghi, A., Cita, M. B., Della Vedova, B., Fusi, N., Mirabile, L., & Pellis, G. (1995). Geophysical evidence of mud diapirism on the Mediterranean Ridge accretionary complex. Marine Geophysical Researches, 17(2), 115-141.

Camerlenghi, A., Cita, M. B., Hieke, W., & Ricchiuto, T. (1992). Geological evidence for mud diapirism on the Mediterranean Ridge accretionary complex. Earth and Planetary Science Letters, 109(3-4), 493-504.

Cita, M. B., RYAN, W. F., & Paggi, L. (1981). Prometheus mud breccia: an example of shale diapirism in the western Mediterranean ridge. In Annales geologiques des Pays helleniques (Vol. 30, pp. 543-570).

Cita, M. B., RYAN, W. F., & Paggi, L. (1981). Prometheus mud breccia: an example of shale diapirism in the western Mediterranean ridge. In Annales geologiques des Pays helleniques (Vol. 30, pp. 543-570).

Dählmann, A., & De Lange, G. J. (2003). Fluid–sediment interactions at Eastern Mediterranean mud volcanoes: a stable isotope study from ODP Leg 160. Earth and Planetary Science Letters, 212(3-4), 377-391.

De Lange, G.J., and Brumsack, H.-J. (1998). Pore-water indications for the occurrence of gas hydrates in Eastern Mediterranean mud dome structures. In Robertson, A.H.F., Emeis, K.-C., Richter, C., and Camerlenghi, A. (Eds.), Proc. ODP, Sci. Results, 160: College Station, TX (Ocean Drilling Program), 569–574.

Dimitrov, L. I. (2002). Mud volcanoes—the most important pathway for degassing deeply buried sediments. Earth-Science Reviews, 59(1-4), 49-76.

Emeis, K.-C, Robertson, A.H.F., Richter, C, et al., (1996). Proceedings of the Ocean Drilling Program, Initial Reports, Vol. 160; Chapter 11. SITE 970

Emeis, K.-C, Robertson, A.H.F., Richter, C, et al., (1996). Proceedings of the Ocean Drilling Program, Initial Reports, Vol. 160; Chapter 12. SITE 971

Espitalié, J., Laporte, J. L., Madec, M., Marquis, F., Leplat, P., Paulet, J., & Boutefeu, A. (1977). Rapid method for source rocks characterization and for determination of petroleum potential and degree of evolution. Revue De L Institut Francais Du Petrole, 32(1), 23-42.

Espitalie, J., Madec, M., Tissot, B., Mennig, J. J., & Leplat, P. (1977, January). Source rock characterization method for petroleum exploration. In Offshore Technology Conference. Offshore Technology Conference.

Fassoulas, C., Kilias, A., & Mountrakis, D. (1994). Postnappe stacking extension and exhumation of high-pressure/low-temperature rocks in the island of Crete, Greece. Tectonics, 13(1), 127-138.

Fusi, N., & Kenyon, N. H. (1996). Distribution of mud diapirism and other geological structures from long-range sidescan sonar (GLORIA) data, in the Eastern Mediterranean Sea. Marine Geology, 132(1-4), 21-38.

Haese, R. R., Hensen, C., & de Lange, G. J. (2006). Pore water geochemistry of eastern Mediterranean mud volcanoes: Implications for fluid transport and fluid origin. Marine Geology, 225(1-4), 191-208.

Hunt, J. M. (1995). Petroleum geochemistry and geology. New York, NY: W.H. Freeman.

Jackson, K. S., Hawkins, P. J., & Bennett, A. J. R. (1980). Regional facies and geochemical evaluation of the southern Denison Trough, Queensland. The APPEA Journal, 20(1), 143-158.

Jiang, C., Chen, Z., Lavoie, D., Percival, J. B., & Kabanov, P. (2017). Mineral carbon MinC (%) from Rock-Eval analysis as a reliable and cost-effective measurement of carbonate contents in shale source and reservoir rocks. Marine and Petroleum Geology, 83, 184-194.

Kidd, R. B., RB, K., MB, C., & WBF, R. (1978). Stratigraphy of eastern Mediterranean sapropel sequences recovered during DSDP Leg 42A and their paleoenvironmental significance.

Kilias, A., Fassoulas, C., & Mountrakis, D. (1993). Tertiary extension of continental crust and uplift of Psiloritis metamorphic core complex at the central part of the Hellenic arc. Bull. Geol. Soc. Greece, 28, 297-314.

Killops, S. D., & Killops, V. J. (2013). Introduction to organic geochemistry. John Wiley & Sons.

Kopf, A., Robertson, A. H. F., & Volkmann, N. (2000). Origin of mud breccia from the Mediterranean Ridge accretionary complex based on evidence of the maturity of organic matter and related petrographic and regional tectonic evidence. Marine Geology, 166(1-4), 65-82.

Le Pichon, X., & Angelier, J. (1979). The Hellenic arc and trench system: a key to the neotectonic evolution of the eastern Mediterranean area. Tectonophysics, 60(1-2), 1-42.

Limonov, A. F., Woodside, J. M., Cita, M. B., & Ivanov, M. K. (1996). The Mediterranean Ridge and related mud diapirism: a background. Marine Geology, 132(1-4), 7-19.

Lourens, L. J., Hilgen, F. J., Shackleton, N. J., Laskar, J., & Wilson, D. (2004). The Neogene Period: 469-471 in. A geologic time scale.

Luterbacher, H. P. (2004). The paleogene period. A geologic time scale 2004, 384-408.

Manutsoglu, E., Soujon, A., & Jacobshagen, V. (2003). Tectonic structure and fabric development of the Plattenkalk unit around the Samaria gorge, Western Crete, Greece. Zeitschrift der Deutschen Geologischen Gesellschaft, 154(1), 85-100.

Marsaglia, K., Tentori, D., Milliken, K., Leckie, R. M., & Doran, L. (2014, October). IODP Digital Reference for Smear Slide Analysis of Marine Mud Part 2: Methodolgy and Atlas of Biogenic Components. In 2014 GSA Annual Meeting in Vancouver, British Columbia.

Martini, E. (1971). Standard Tertiary and Quaternary calcareous nannoplankton zonation. In Proc. II Planktonic Conference, Roma 1970, Roma, Tecnoscienza (Vol. 2, pp. 739-785).

Mascle, J., Mary, F., Praeg, D., Brosolo, L., Camera, L., Ceramicola, S., & Dupré, S. (2014). Distribution and geological control of mud volcanoes and other fluid/free gas seepage features in the Mediterranean Sea and nearby Gulf of Cadiz. Geo-Marine Letters, 34(2-3), 89-110.

Mountrakis, D. (2002). Tectonic evolution of the Hellenic orogen: Geometry and kinematics of deformation. Bull. Geol. Soc. Greece, 34(6), 2113-2126.

Okada, H. & Bukry, D. 1980: Supplementary modification and introduction of code numbers to the low-latitude coccolith biostratigraphic zonation (Bukry 1973; 1975). Marine Micropaleontology 5, 321–325

Panagiotopoulos, I. P., Paraschos, F., Rousakis, G., Hatzianestis, I., Parinos, C., Morfis, I., & Gogou, A. (2020). Assessment of the eruptive activity and identification of the mud breccia's source in the Olimpi mud volcano field, Eastern Mediterranean. Deep Sea Research Part II: Topical Studies in Oceanography, 171, 104701.

Perissoratis, C., Ioakim, C., Alexandri, S., Woodside, J., Nomikou, P., Dählmann, A. & Lykousis, V. (2011). Thessaloniki mud volcano, the shallowest gas hydrate-bearing mud volcano in the Anaximander Mountains, Eastern Mediterranean. Journal of Geological Research, 2011.

Peters, K. E. (1986). Guidelines for evaluating petroleum source rock using programmed pyrolysis. AAPG bulletin, 70(3), 318-329.

Peters, K. E., Walters, C. C., & Moldowan, J. M. (2005). Biomarkers and isotopes in petroleum exploration and earth history. The Biomarker Guide, 2, 700.

Robertson, A. H., & Kopf, A. (1998). Tectonic setting and processes of mud volcanism on the Mediterranean Ridge accretionary complex: evidence from Leg 160. Proceedings of the Ocean Drilling Program, Scientific Results, Vol. 160; Chapter 50.

Schulz, H. M., Emeis, K. C., & Volkmann, N. (1997). Organic carbon provenance and maturity in the mud breccia from the Napoli mud volcano: Indicators of origin and burial depth. Earth and planetary science letters, 147(1-4), 141-151.

Silva, I. P., Erba, E., Spezzaferri, S., & Cita, M. B. (1996). Age variation in the source of the diapiric mud breccia along and across the axis of the Mediterranean Ridge Accretionary Complex. Marine geology, 132(1-4), 175-202.

Staffini, F., Spezzaferri, S., & Aghib, F. (1993). Mud diapirs of the Mediterranean Ridge: sedimentological and micropaleontological study of the mud breccia. Rivista italiana di paleontologia e stratigrafia, 99(2).

Taylforth, J. E., McCay, G. A., Ellam, R., Raffi, I., Kroon, D., & Robertson, A. H. (2014). Middle Miocene (Langhian) sapropel formation in the easternmost Mediterranean deep-water basin: Evidence from northern Cyprus. Marine and Petroleum Geology, 57, 521-536.

Tissot, B. P., & Welte, D. H. (2013). Petroleum formation and occurrence. Springer Science & Business Media.

Triantaphyllou, M. V. (2013). Calcareous nannofossil dating of Ionian and Gavrovo flysch deposits in the External Hellenides Carbonate Platform (Greece): Overview and implications. Tectonophysics, 595, 235-249.

Waples, D. W. (2013). Geochemistry in petroleum exploration. Springer Science & Business Media.

Woodside, J. M., Ivanov, M. K., & Limonov, A. F. (1998). Shallow gas and gas hydrates in the Anaximander Mountains region, eastern Mediterranean Sea. Geological Society, London, Special Publications, 137(1), 177-193.

Woodside, J.M., Ivanov, M.K., Limonov, A.F., (Eds.), 1997. Neotectonics and fluid flow through seafloor sediments in the Eastern Mediterranean and Black Seas—Parts I and II. IOC Tech. Ser. 48.

Appendix

For each mud structure, tables were constructed with all the available information, extracted from the samples' study. The tables include:

- sample code and sampling interval
- age of the sediments,
- percentage of nannofossils observed in the microscopical image
- rock type and macroscopical observations
- Rock-Eval pyrolysis measured parameters (S1, S2, S3, TOC, MINC and Tmax)
- Rock-Eval pyrolysis calculated parameters (HI, OI and carbonate content)

In addition, calcareous nannoplankton study results were plotted for each mud structure and each sample. The tables include nannofossil assemblages indicative of a geological era (e.g. Neogene, Paleogene etc.) and the absolute abundance of each nannofossil recorded.

Gelendzhik MV

	MVs	interval (cm)	type	nanno (%)	Age	rock type	Consolidation	colour	comments	OI	HI	Tmax (°C)	TOC (%)	MINC (%)	S1 (mg/g)	S2 (mg/g)	S3 (mg/g)	carbonate content (%)
Gelendzhik	LEV 1c GC	4 - 6	*matrix*	30	Mixed Oligocene-Miocene	sandy mud		light yelowish brown	Quartz sound	228,09	39,33	421	0,89	1,85	0,01	0,35	2,03	14,76
	LEV 1c GC	4 - 6	clast 1	70 - 80	NN7	mudstone	soft	yellowish-greyish white		91,09	437,62	413	2,02	4,66	0,39	8,84	1,84	37,17
	LEV 1c GC	4 - 6	clast 2	10	NN7	mudstone	semi - well	dark-very dark grey		331,15	114,75		0,61	0,35	0,01	0,70	2,02	2,79
	LEV 1c GC	18 - 20	*matrix*	30	Mixed Oligocene-Miocene	sandy mud		light yelowish brown	Quartz sound	366,04	58,49	426	0,53	1,24	0,01	0,31	1,94	9,89
	LEV 1c GC	18 - 20	clast 1	50	NN6	mudstone	semi	greenish grey		95,38	155,38		0,65	0,36	0,00	1,01	0,62	2,87
	LEV 1c GC	65 - 67	*matrix*	30	Mixed Oligocene-Miocene	sandy mud		light yelowish brown		431,91	87,23		0,47	1,01	0,02	0,41	2,03	8,06
	LEV 1c GC	65 - 67	clast 1	<10	NN7	mudstone	semi	grey-dark grey		354,00	116,00		0,50	0,80	0,02	0,58	1,77	6,38

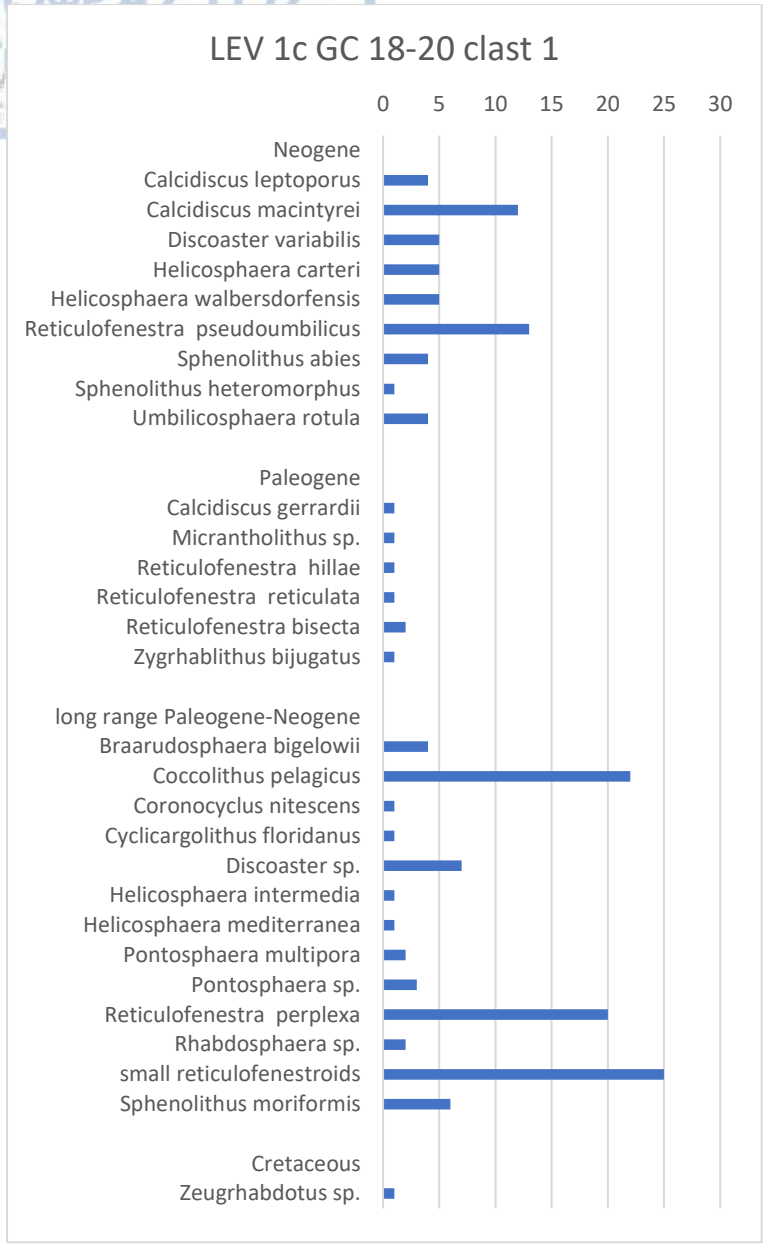

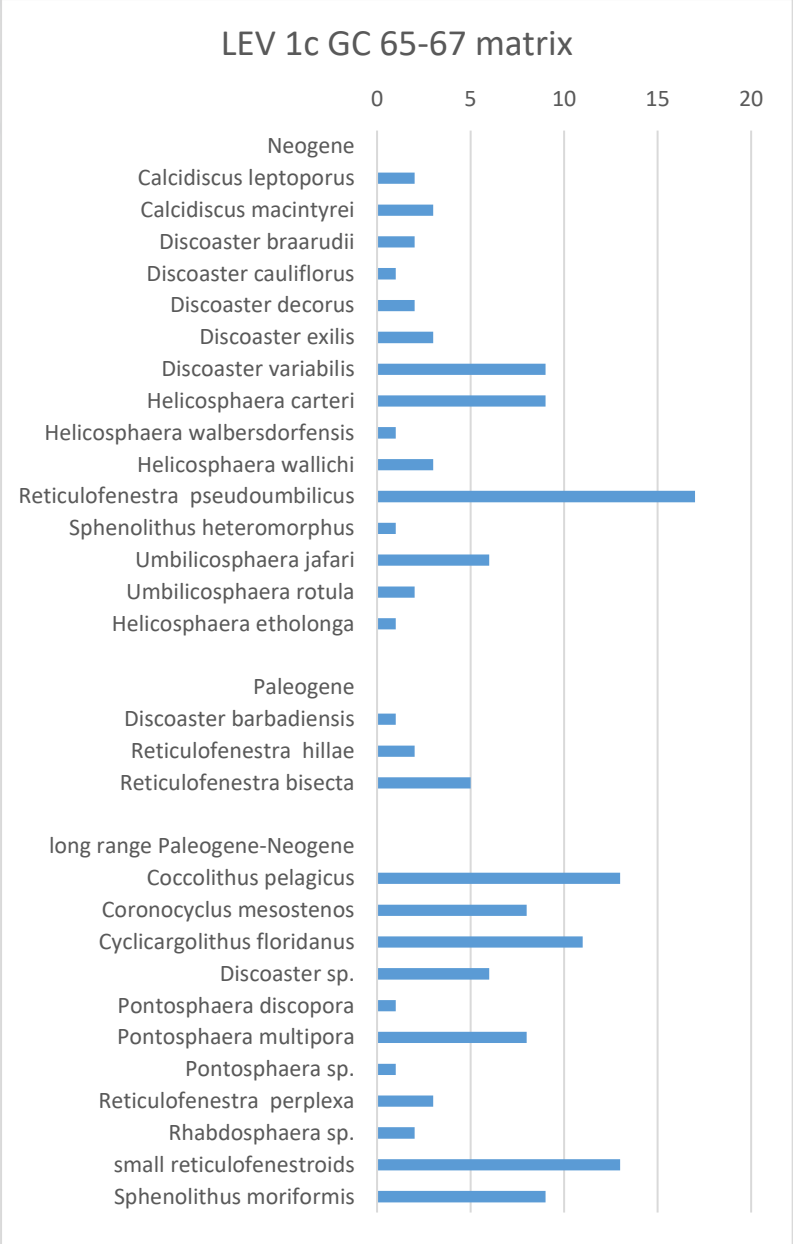

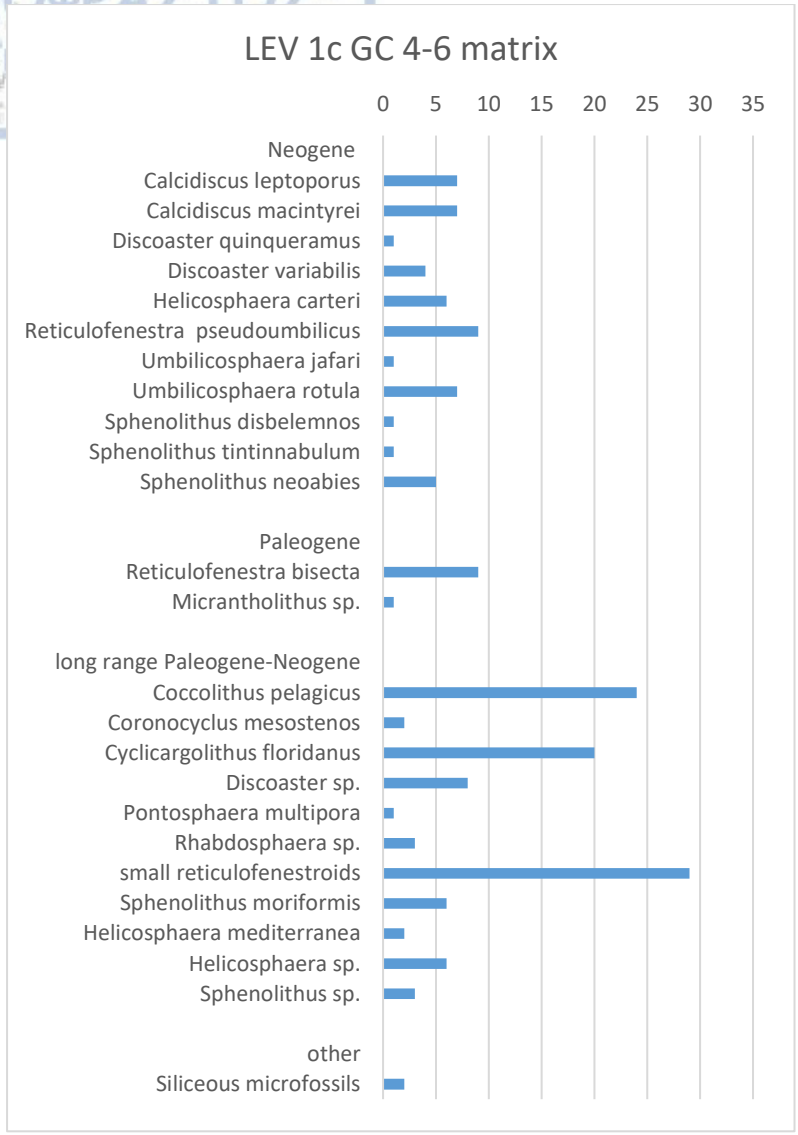

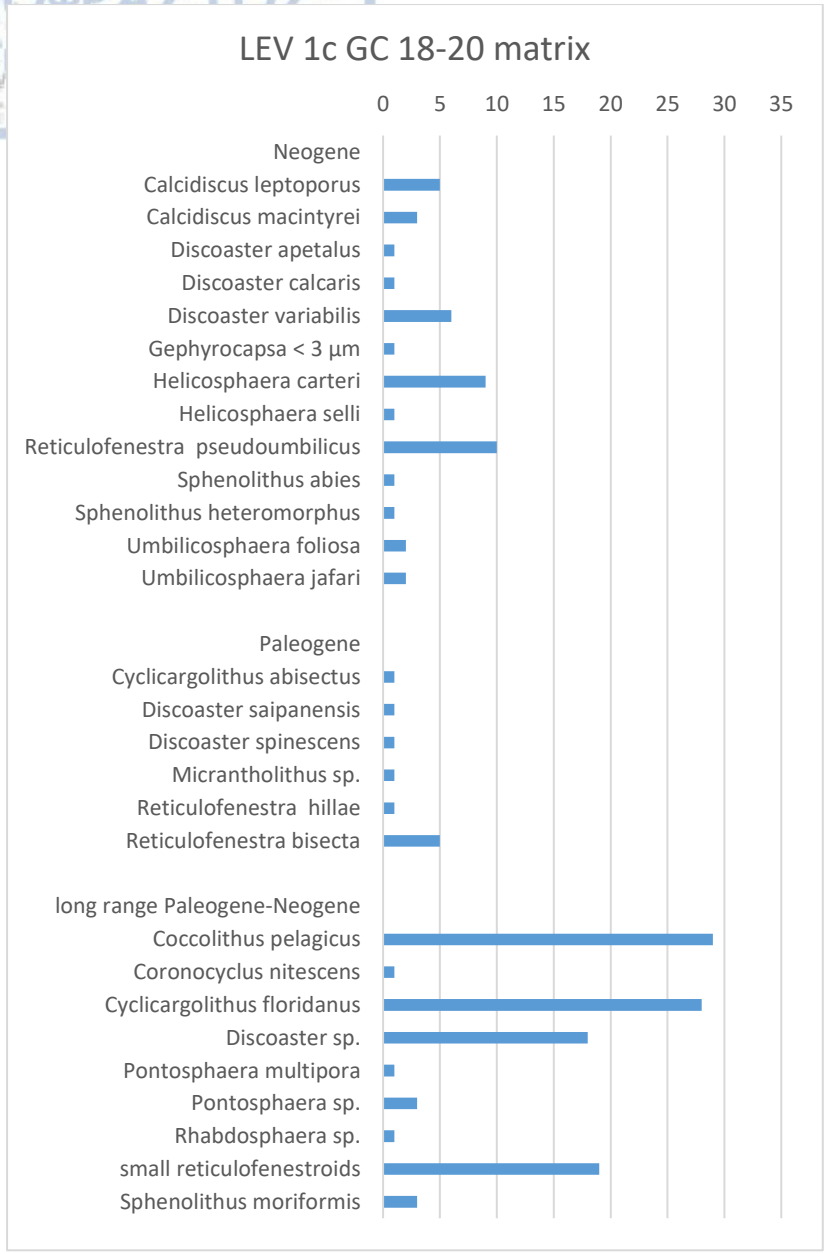

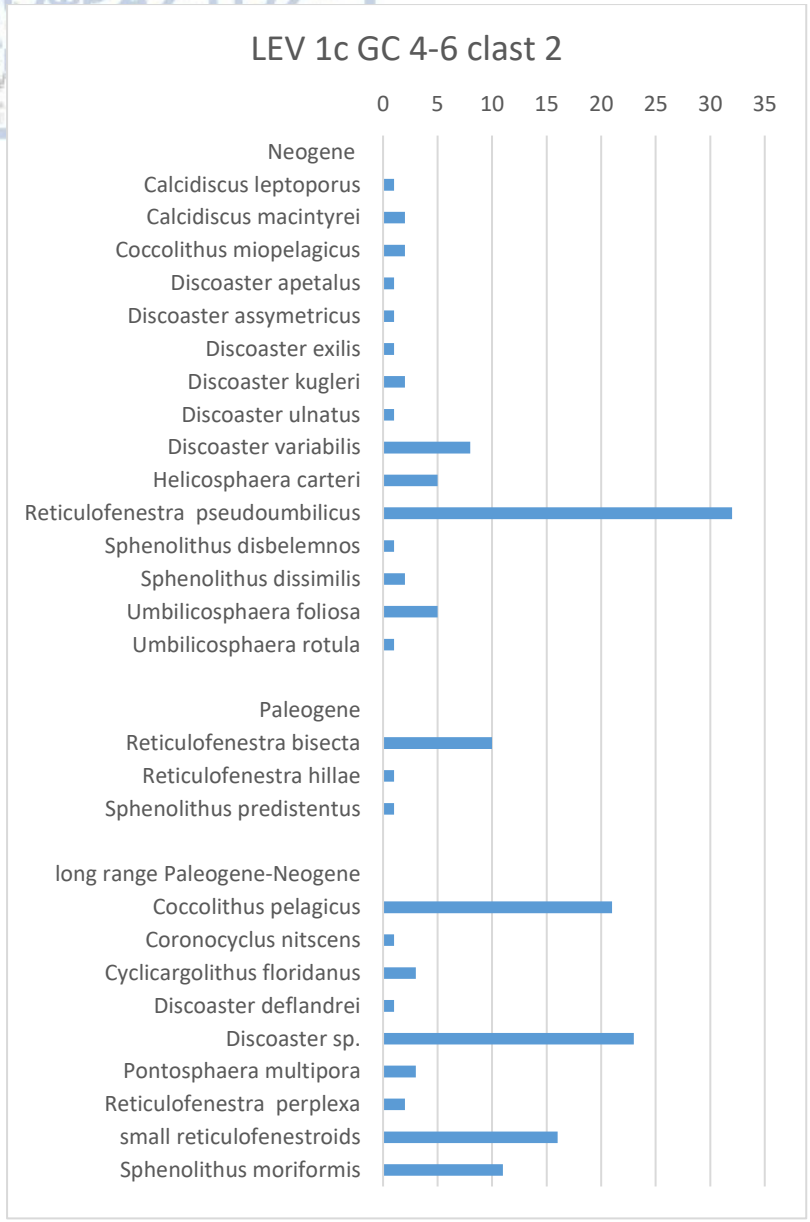

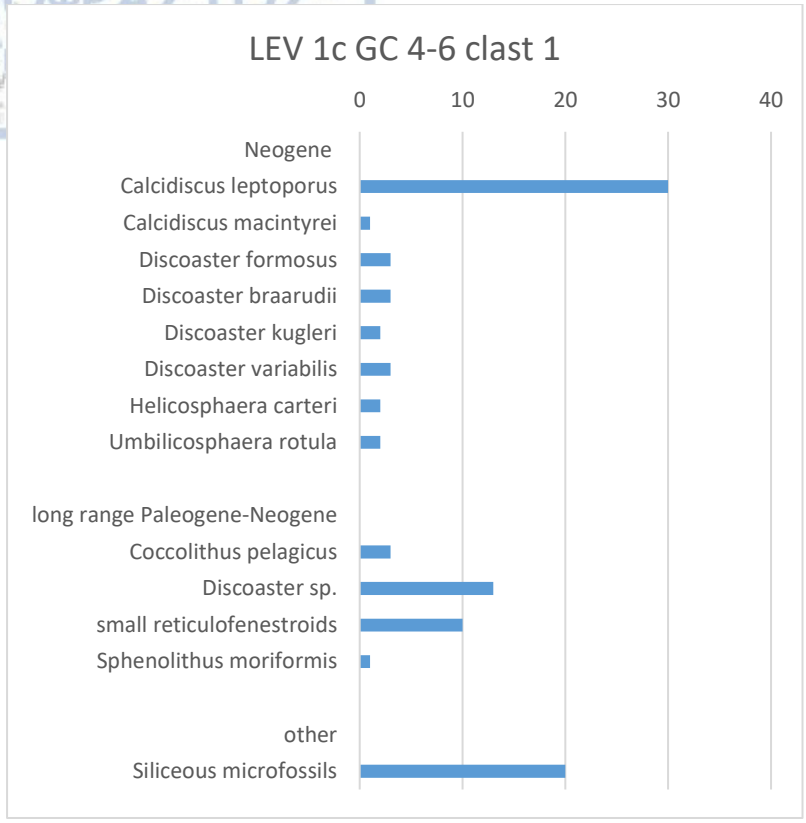

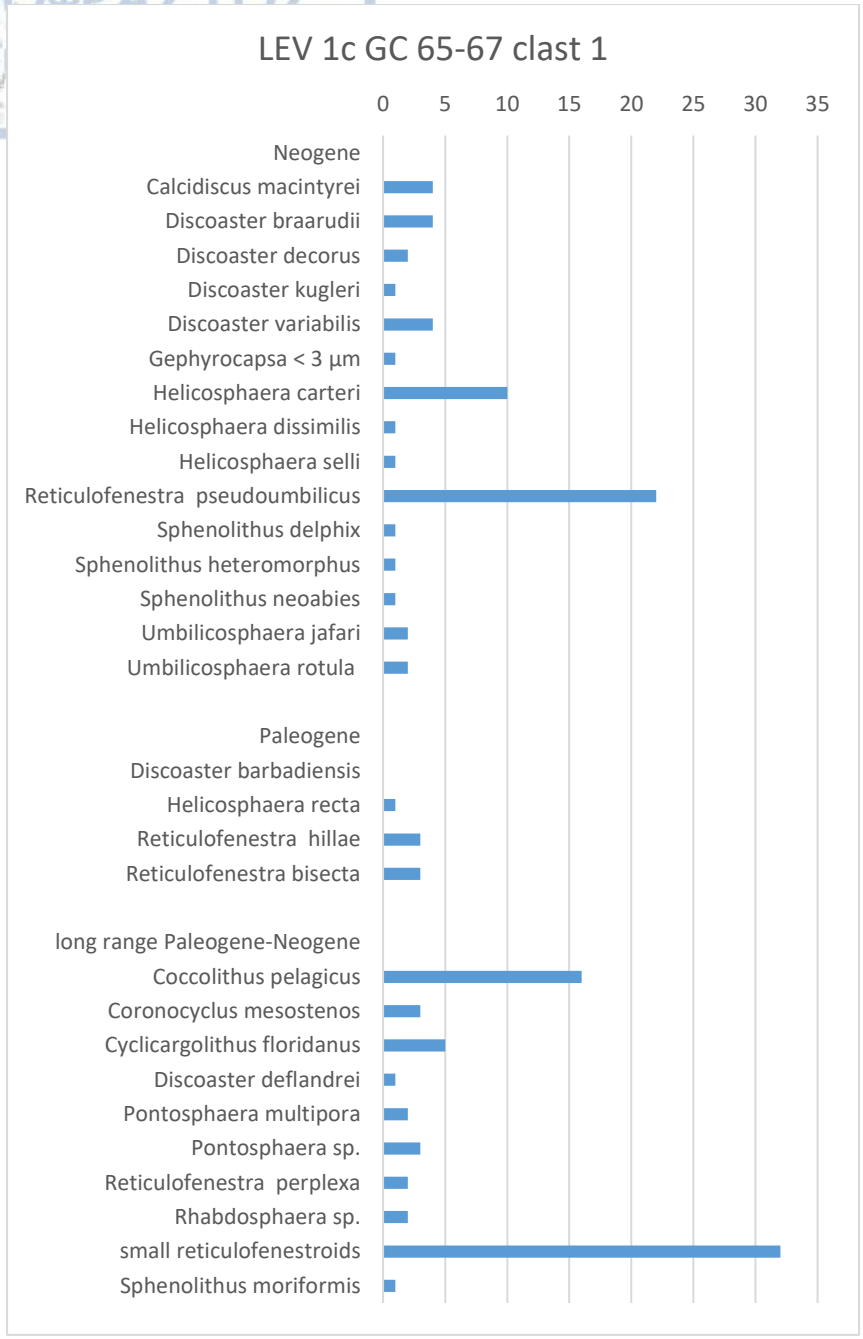

Heraklion MV

	MVs	interval (cm)	type	nanno (%)	Age	rock type	Consolidation	colour	comments	OI	HI	Tmax (°C)	TOC (%)	MINC (%)	S1 (mg/g)	S2 (mg/g)	S3 (mg/g)	carbonate content (%)
Heraklion	LEV 3c GC	2 - 5	*matrix*	almost barren	undetermined	sandy mud		light yelowish brown	Quartz sound	32,00	200,00		0,25	0,06	0,00	0,50	0,08	0,48
	LEV 3c GC	25 - 27	*matrix*	30	Mixed Oligocene-Miocene	sandy mud		light yelowish brown	Quartz sound	138,30	34,04	418	0,94	2,80	0,01	0,32	1,30	22,33
	LEV 3c GC	65 - 67	clast 1	30-40	NN4	mudstone	soft	yellowish-greyish white		126,80	131,96	434	0,97	5,04	0,01	1,28	1,23	40,20
	LEV 3c GC	65 - 67	clast 2	?	undetermined	?	soft	light grey		142,67	41,33	416	0,75	4,59	0,00	0,31	1,07	36,61

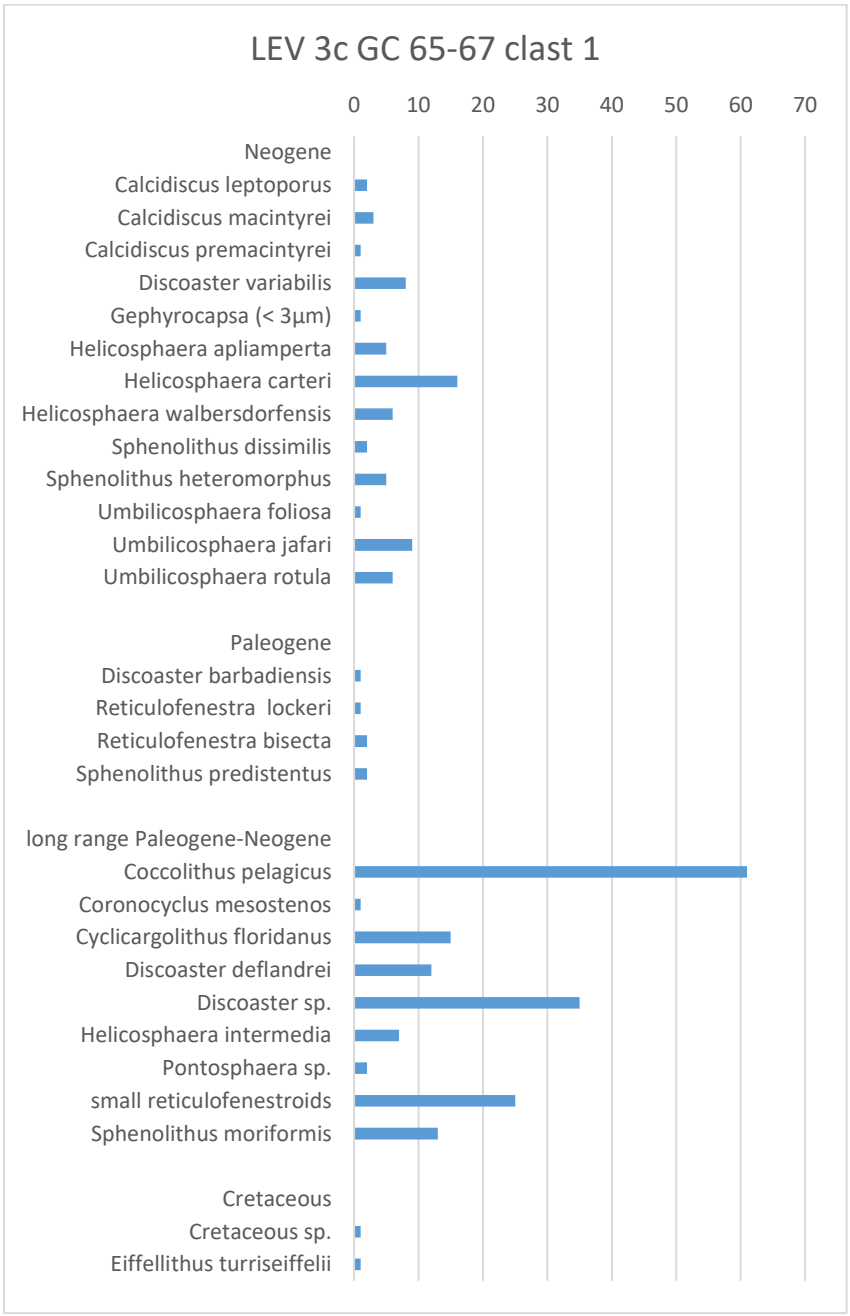

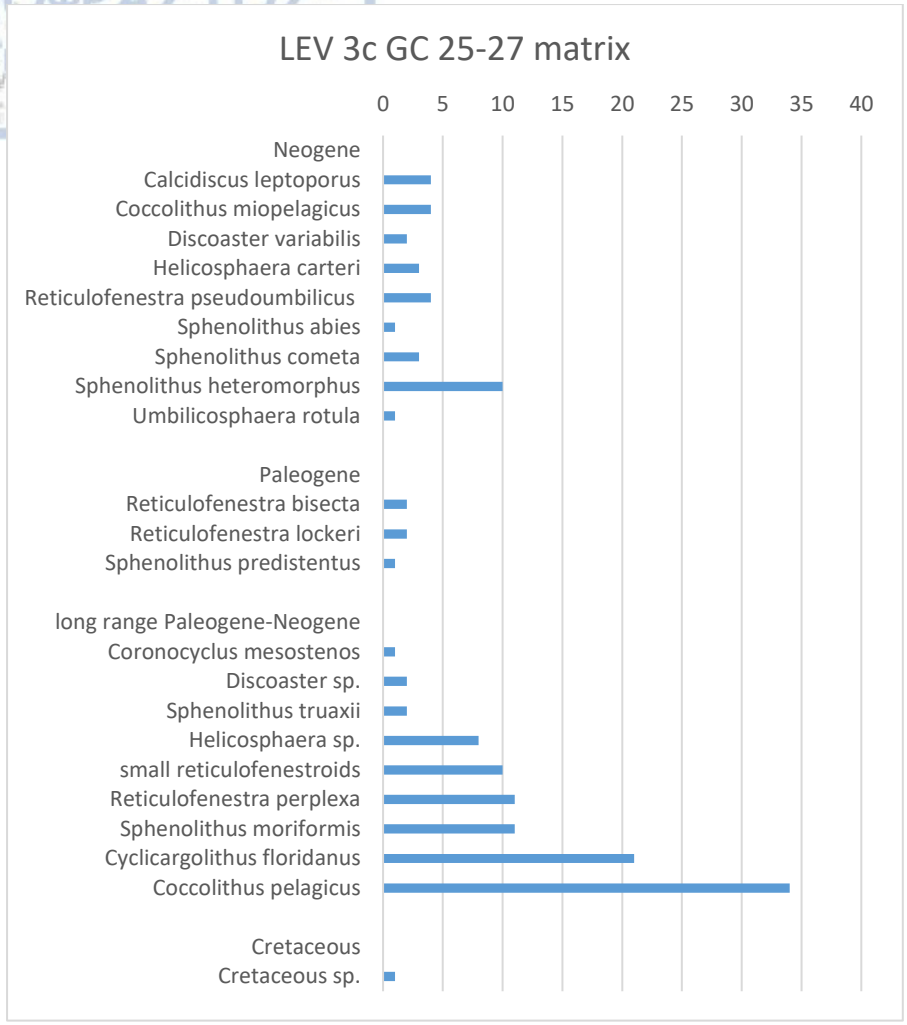

Moscow MV

	MVs	interval (cm)	type	nanno (%)	Age	rock type	Consolidation	colour	comments	OI	HI	Tmax (°C)	TOC (%)	MINC (%)	S1 (mg/g)	S2 (mg/g)	S3 (mg/g)	carbonate content (%)
Moscow	LEV 5b GC	10 - 12	*matrix*	30	Mixed Oligocene-Miocene	sandy mud		light yelowish brown	Quartz sound	529,41	35,29	426	0,34	2,68	0,00	0,12	1,80	21,38
	LEV 5b GC	10 - 12	clast 1	≈ 10	Mixed Oligocene-Miocene (NP24-NP25?)	shale	semi	greenish grey	subparallel fissility	516,67	58,33	419	0,36	2,46	0,00	0,21	1,86	19,62
	LEV 5b GC	10 - 12	clast 2	≈ 30	Mixed Oligocene-Miocene (NN4?)	mudstone	semi	dark grey		481,82	145,45		0,11	0,18	0,01	0,16	0,53	1,44
	LEV 5b GC	40 - 42	clast 1	70-80	NP24	mudstone	semi - soft	yellowish white		465,79	21,05	427	0,38	6,04	0,00	0,08	1,77	48,18
	LEV 5b GC	40 - 42	clast 2	≈ 10	Mixed Oligocene-Miocene	mudstone	semi - well	dark grey-black		373,68	100,00		0,19	0,26	0,00	0,19	0,71	2,07
	LEV 5b GC	70 - 72	clast 1	30-40	NN4	carbonate mudstone		light grey-grey		230,59	220,00	433	0,85	6,71	0,02	1,87	1,96	53,52
	LEV 5b GC	100 - 102	*matrix*	30	Mixed Oligocene-Miocene	sandy mud		light yelowish brown	Quartz sound	490,91	57,58	424	0,33	1,93	0,00	0,19	1,62	15,39
	LEV 5b GC	100 - 102	clast 1	≤ 10	Mixed Oligocene-Miocene (NP23-NP24?)	mudstone	semi	dark grey		287,50	64,58	426	0,48	0,43	0,00	0,31	1,38	3,43
	LEV 5b GC	100 - 102	clast 2	20-30	NN7	mudstone	semi - well	light grey-grey		195,83	91,67	423	0,24	1,16	0,00	0,22	0,47	9,25
	LEV 5b GC	123 - 125	*matrix*	30	Mixed Oligocene-Miocene	sandy mud		light yelowish brown	Quartz sound	497,14	68,57	427	0,35	1,93	0,01	0,24	1,74	15,39
	LEV 5b GC	123 - 125	clast 1	almost barren	undetermined	mudstone	semi	dark brownish grey		249,12	61,40		0,57	0,22	0,02	0,35	1,42	1,75
	LEV 5b GC	123 - 125	clast 2	30	NN5	carbonate mudstone	semi - well	light yellowish white		539,13	17,39		0,23	8,23	0,01	0,04	1,24	65,64

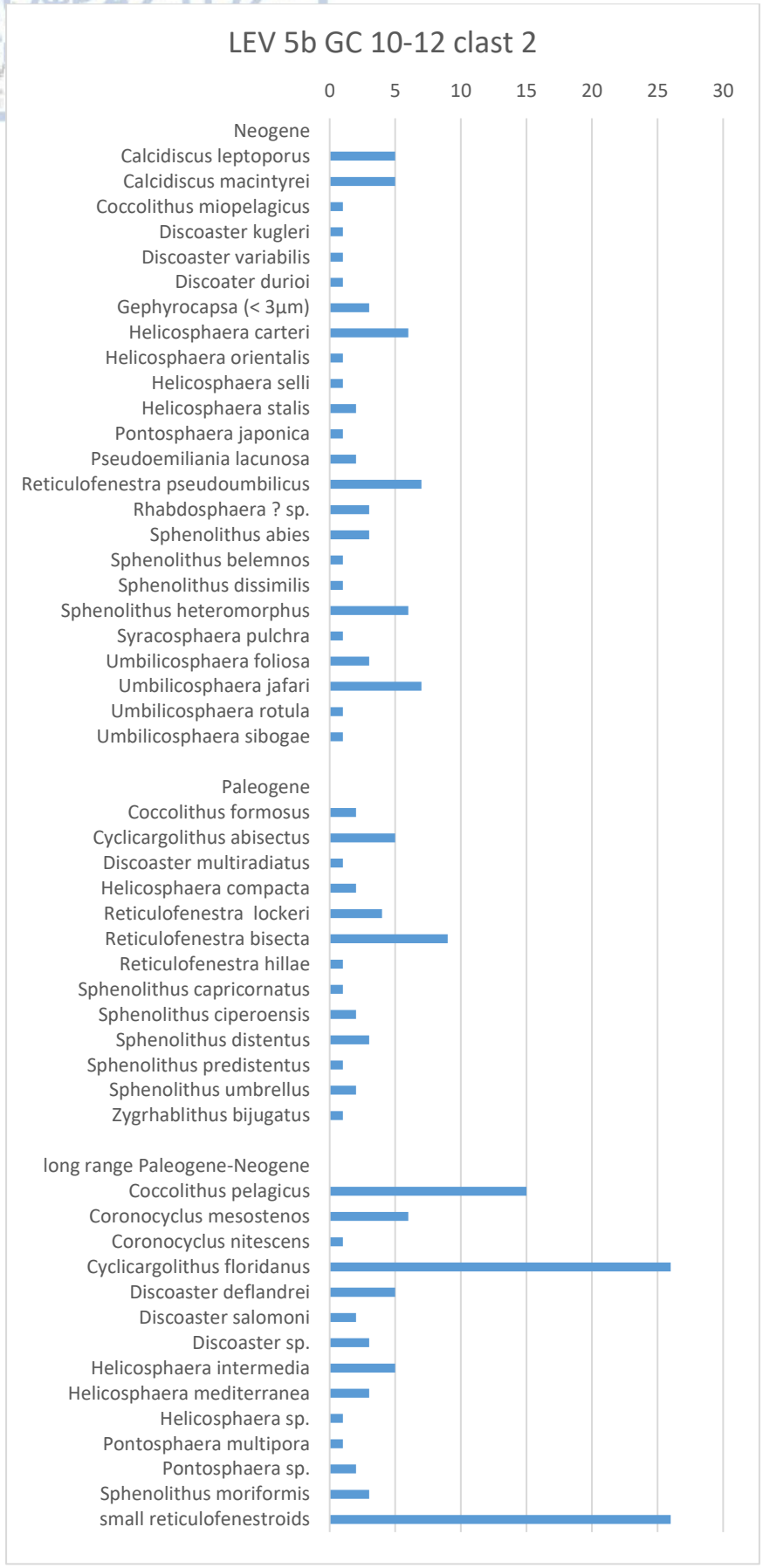

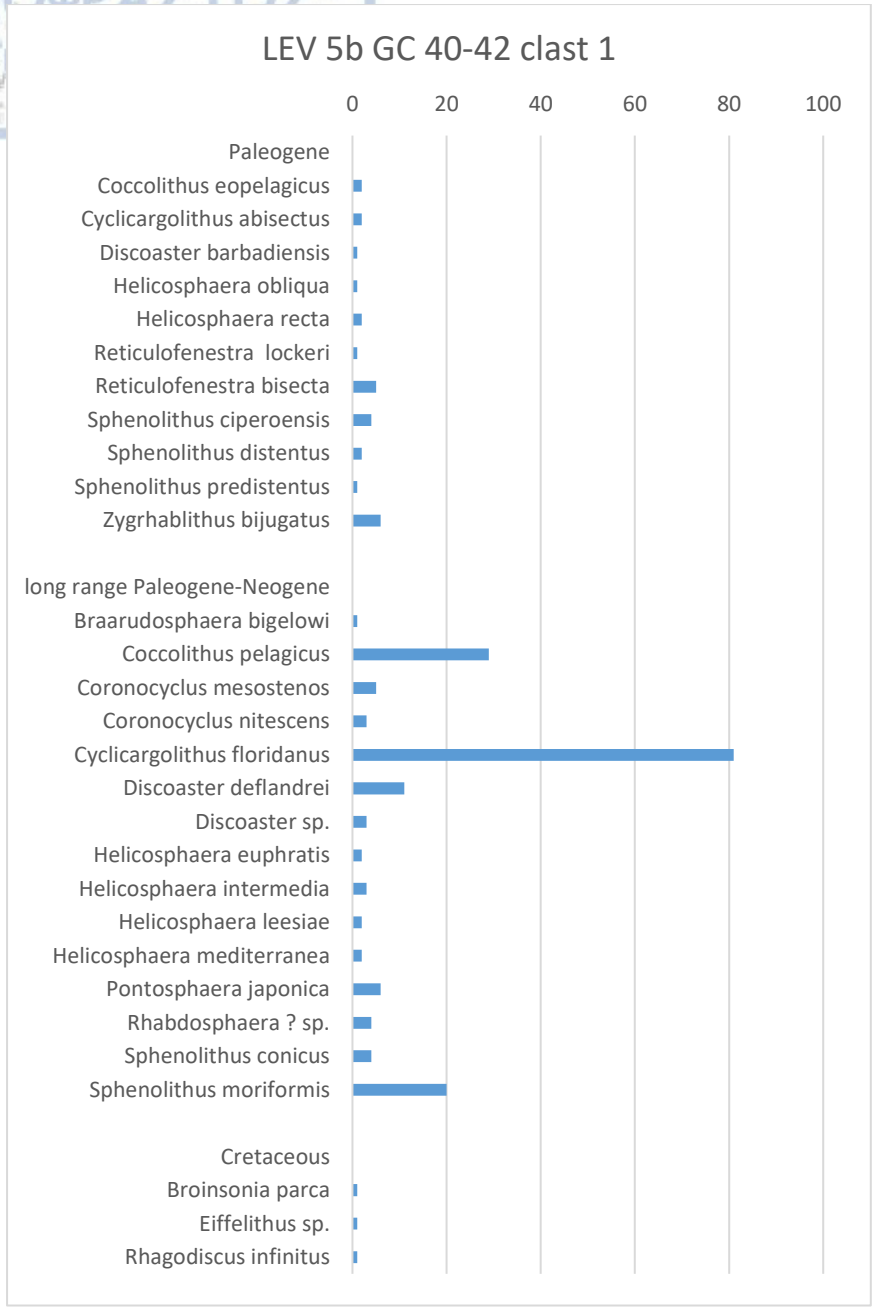

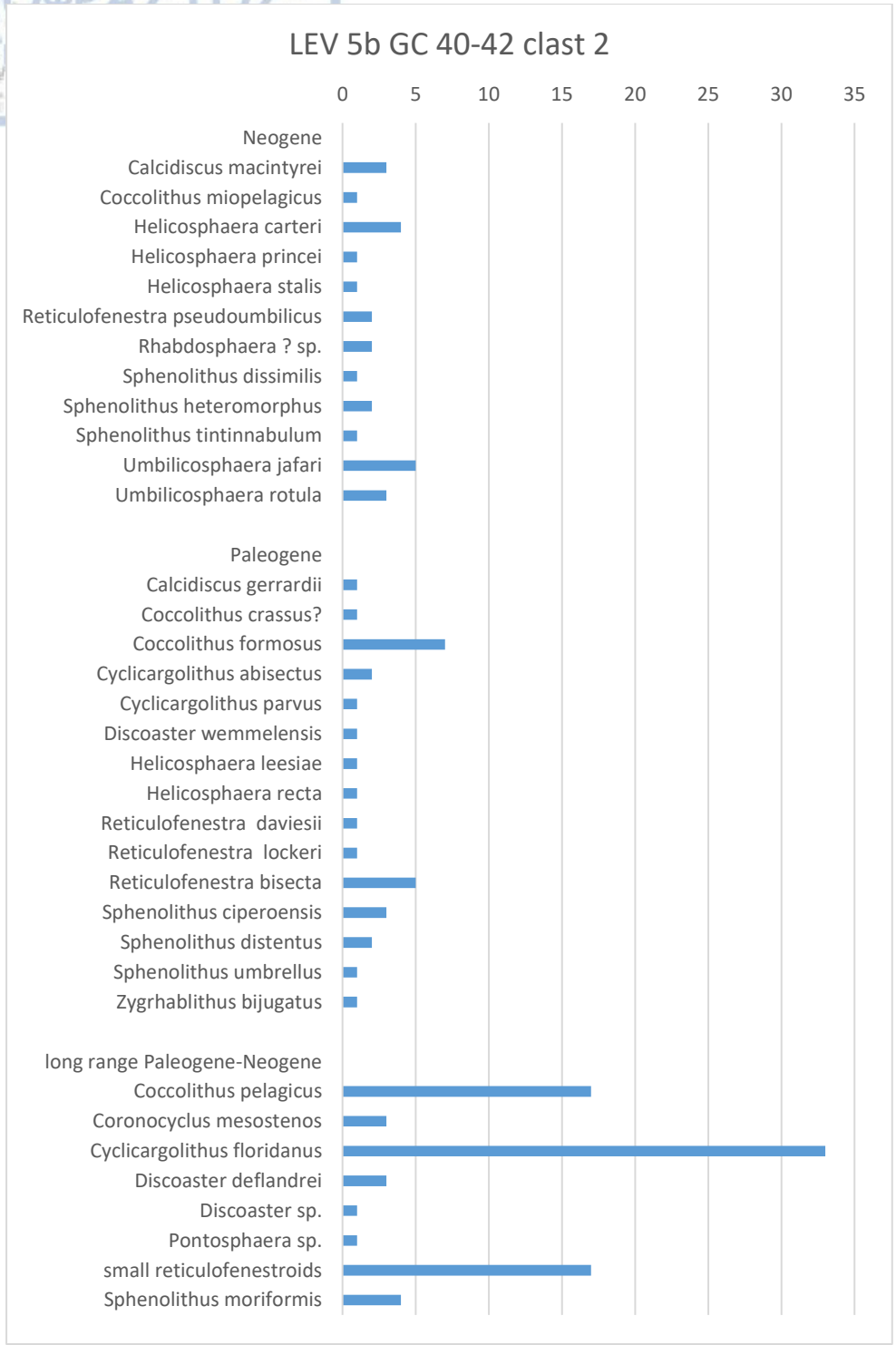

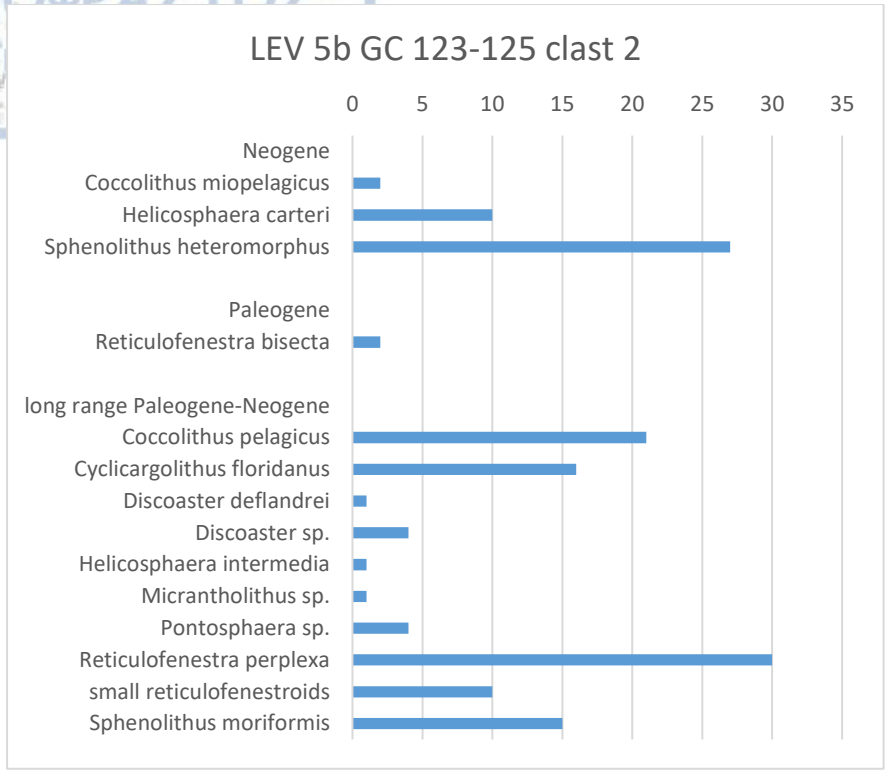

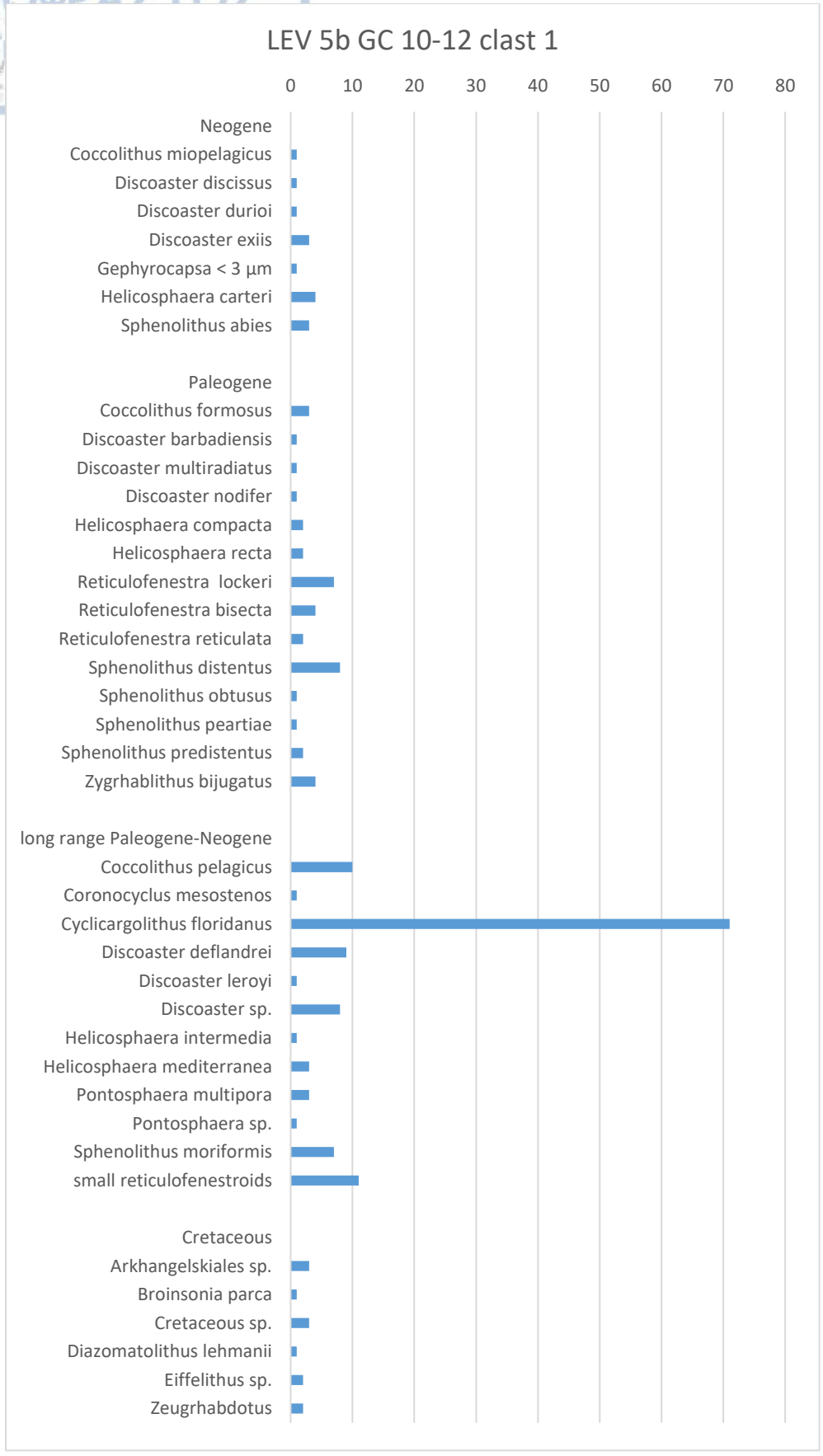

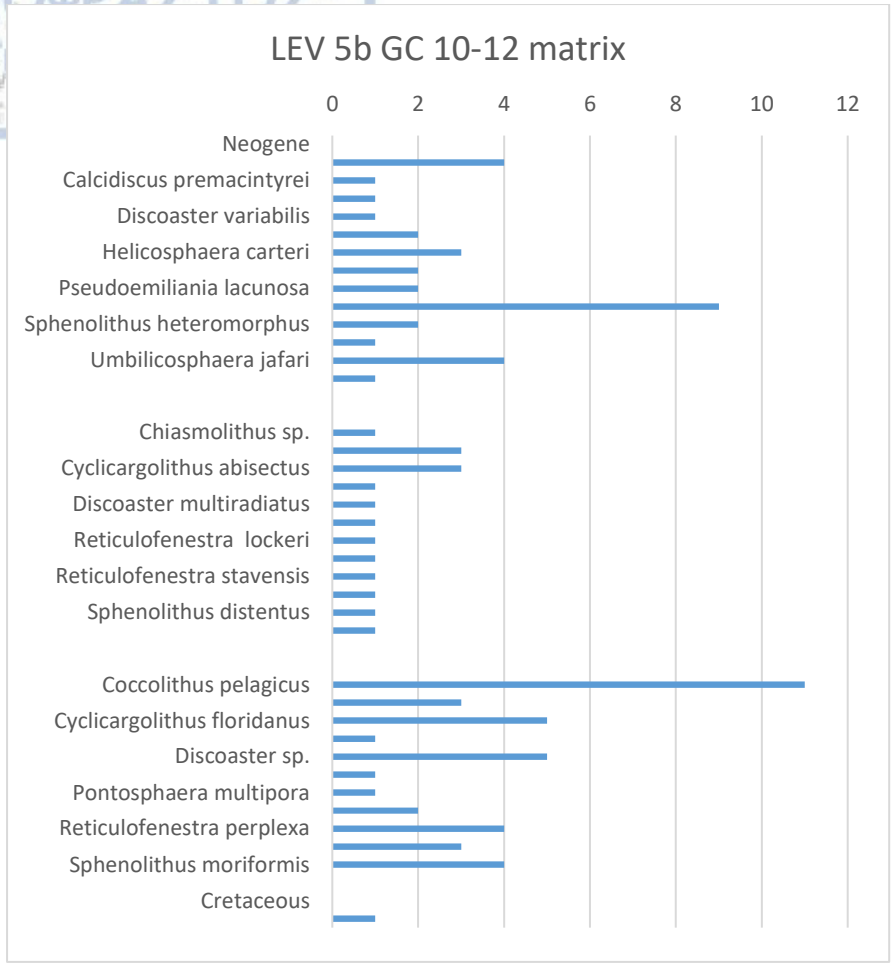

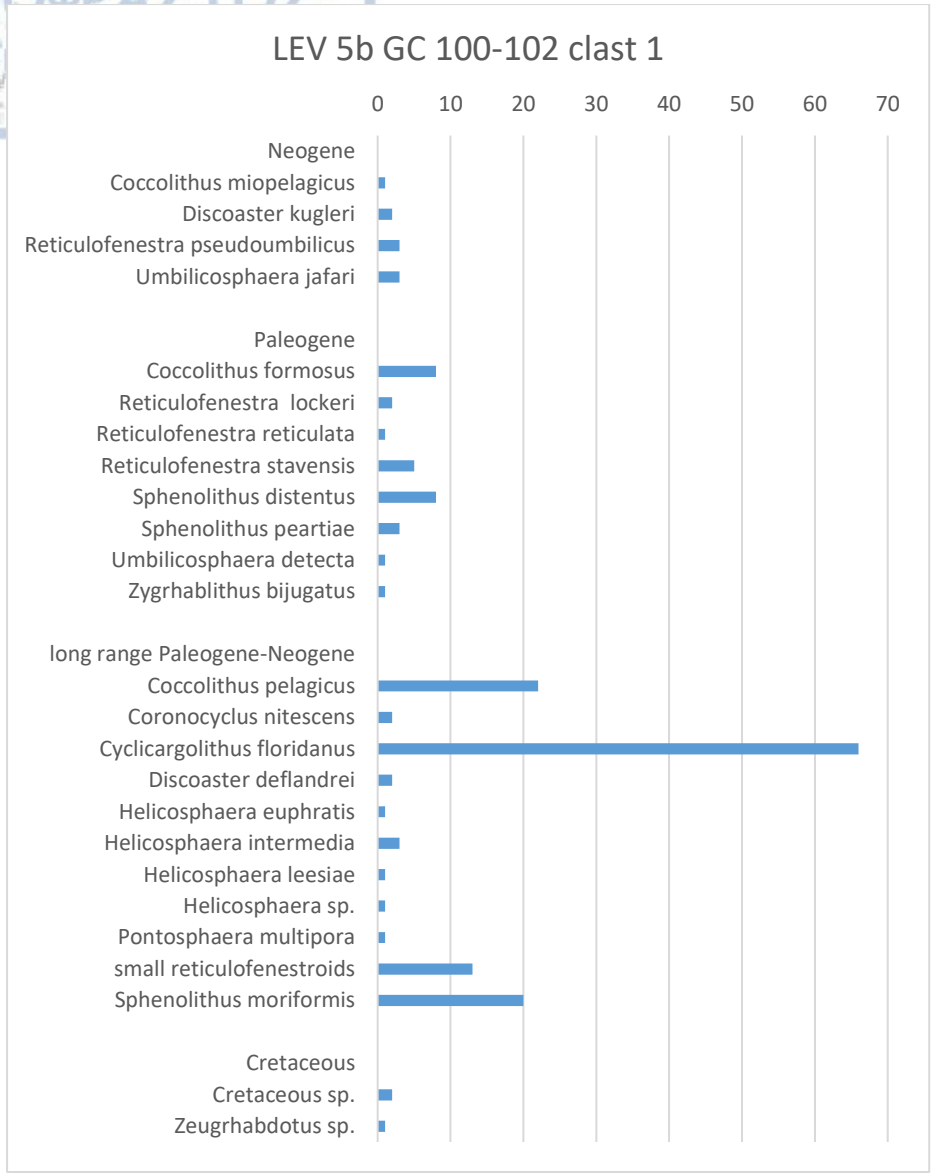

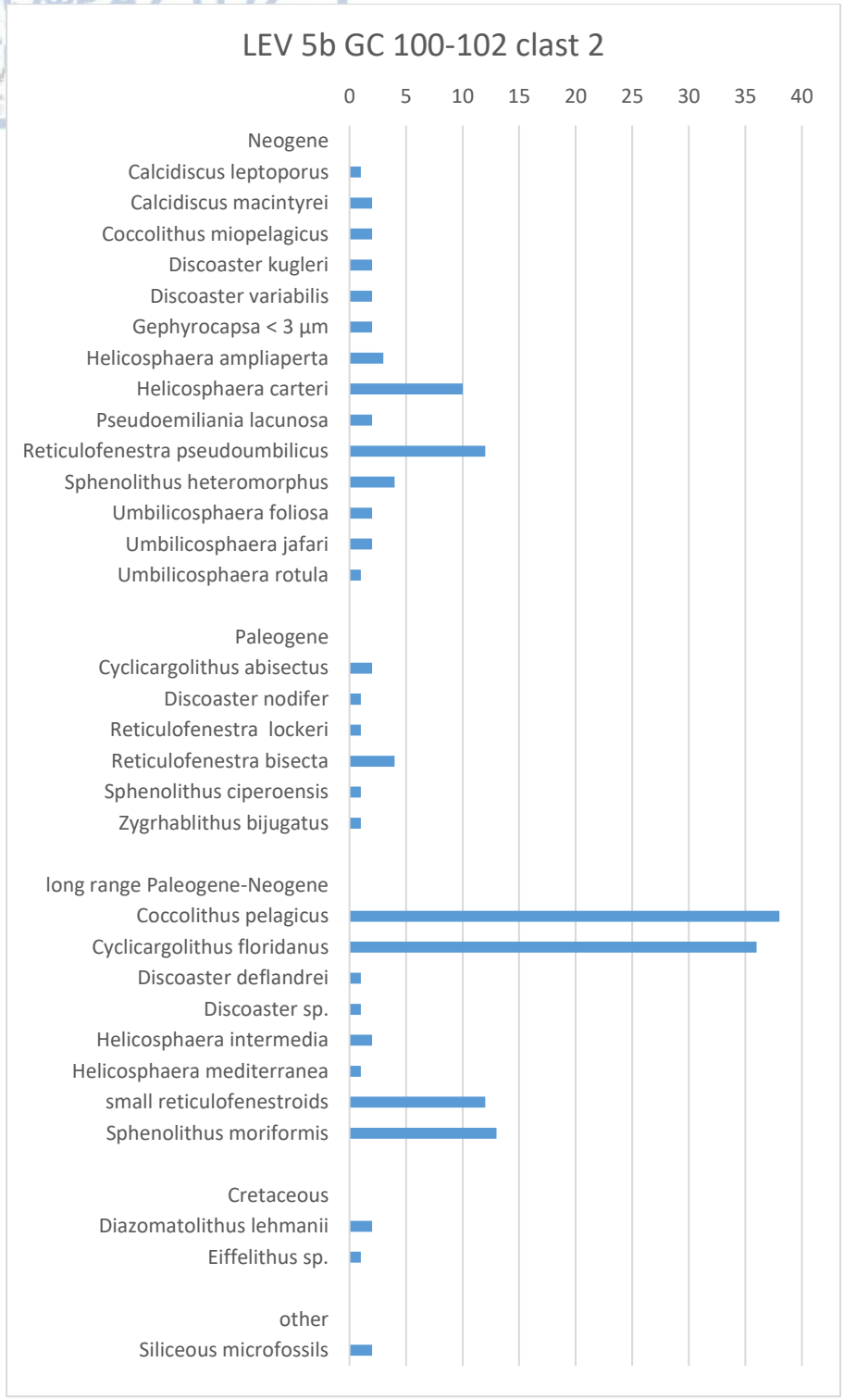

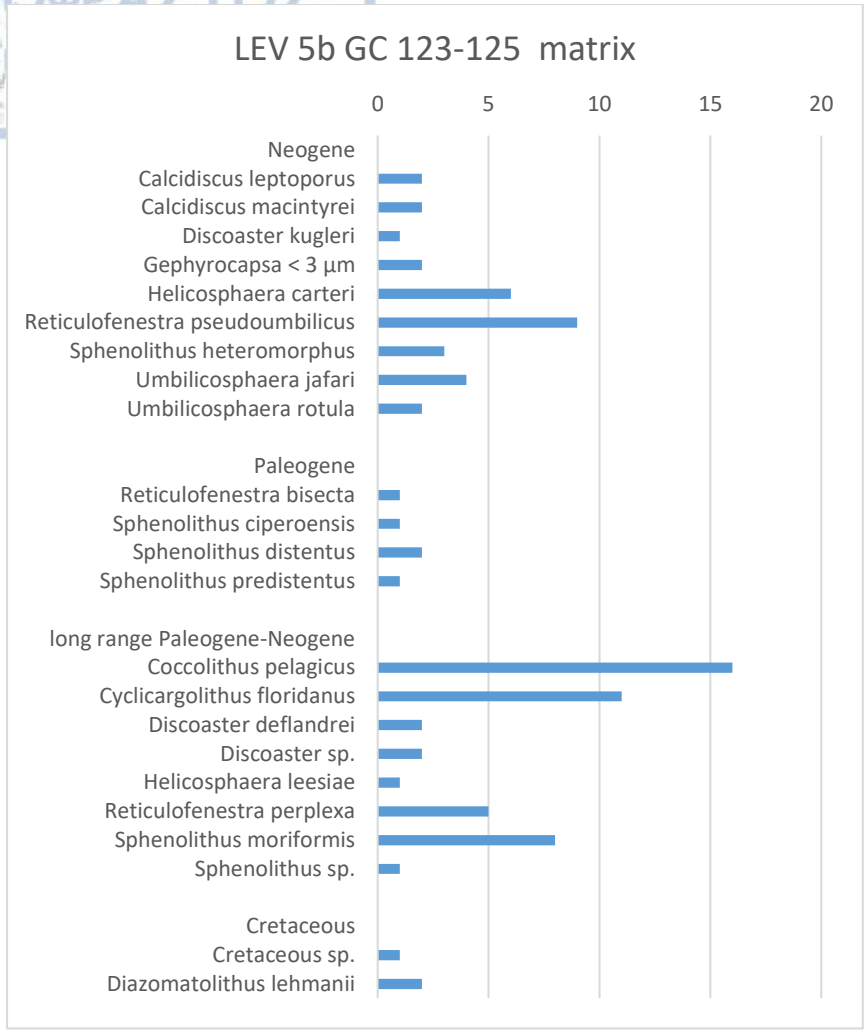

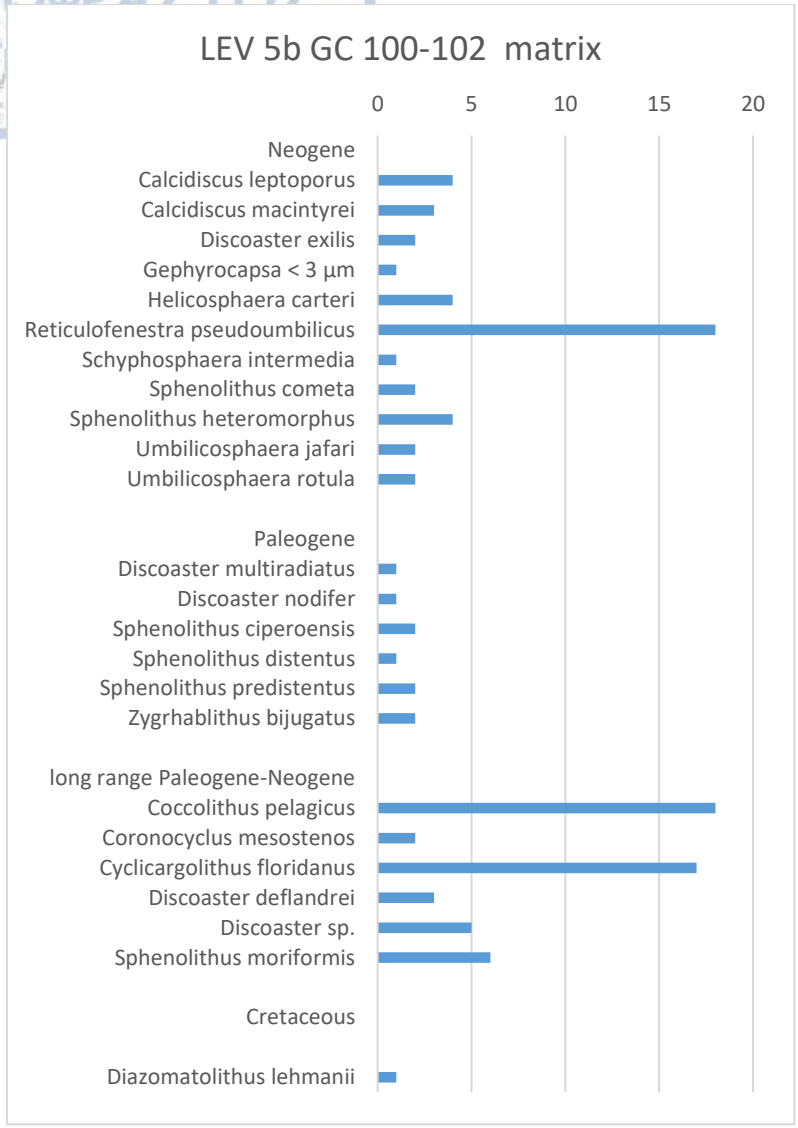

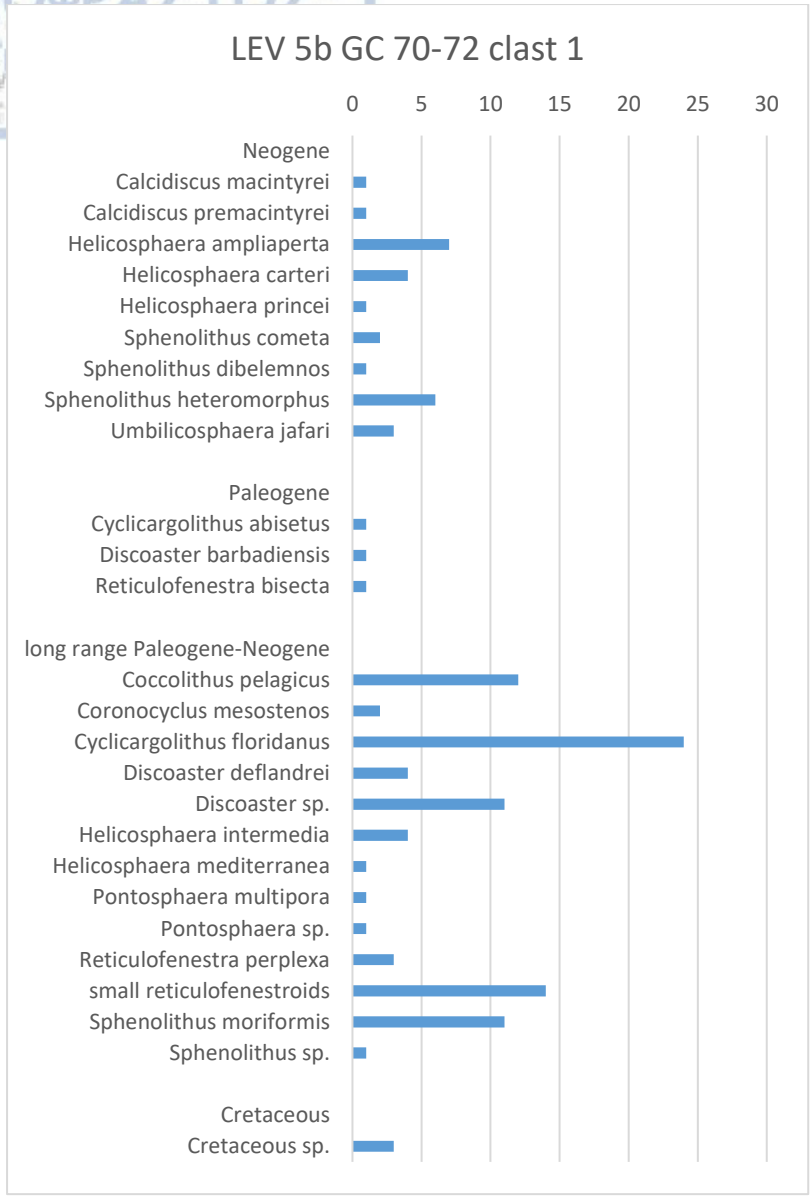

Milano MV

	MVs	interval (cm)	type	nanno (%)	Age	rock type	Consolidation	colour	comments	OI	HI	Tmax (°C)	TOC (%)	MINC (%)	S1 (mg/g)	S2 (mg/g)	S3 (mg/g)	carbonate content (%)
Milano	LEV 7b GC	12 - 14	*matrix*	30	Mixed Oligocene-Miocene	sandy mud		light yelowish brown	Quartz sound	473,17	58,54	427	0,41	1,64	0,01	0,24	1,94	13,08
	LEV 7b GC	40 - 43	*matrix*	30	Mixed Oligocene-Miocene	sandy mud		light yelowish brown	Quartz sound	446,94	67,35	427	0,49	1,67	0,01	0,33	1,94	13,32
	LEV 7b GC	40 - 43	clast 1	< 10	NN6	shale	well	dark brownish grey	parallel fissility	270,49	88,52		0,61	0,40	0,01	0,54	1,65	3,19
	LEV 7b GC	40 - 43	clast 2	20-30	NN6	mudstone	semi	greenish grey		554,17	37,50	399	0,48	2,29	0,01	0,18	2,66	18,27
	LEV 7b GC	78 - 80	*matrix*	30	Mixed Oligocene-Miocene	sandy mud		light yelowish brown	Quartz sound	380,43	65,22	432	0,46	1,72	0,01	0,30	1,75	13,72
	LEV 7b GC	78 - 80	clast 1	< 5	NN6	mudstone		dark grey		265,71	42,86	427	0,35	1,46	0,00	0,15	0,93	11,64
	LEV 7b GC	78 - 80	clast 2 ?	almost barren	undetermined	mudstone				477,27	52,27	413	0,44	0,62	0,01	0,23	2,10	4,95

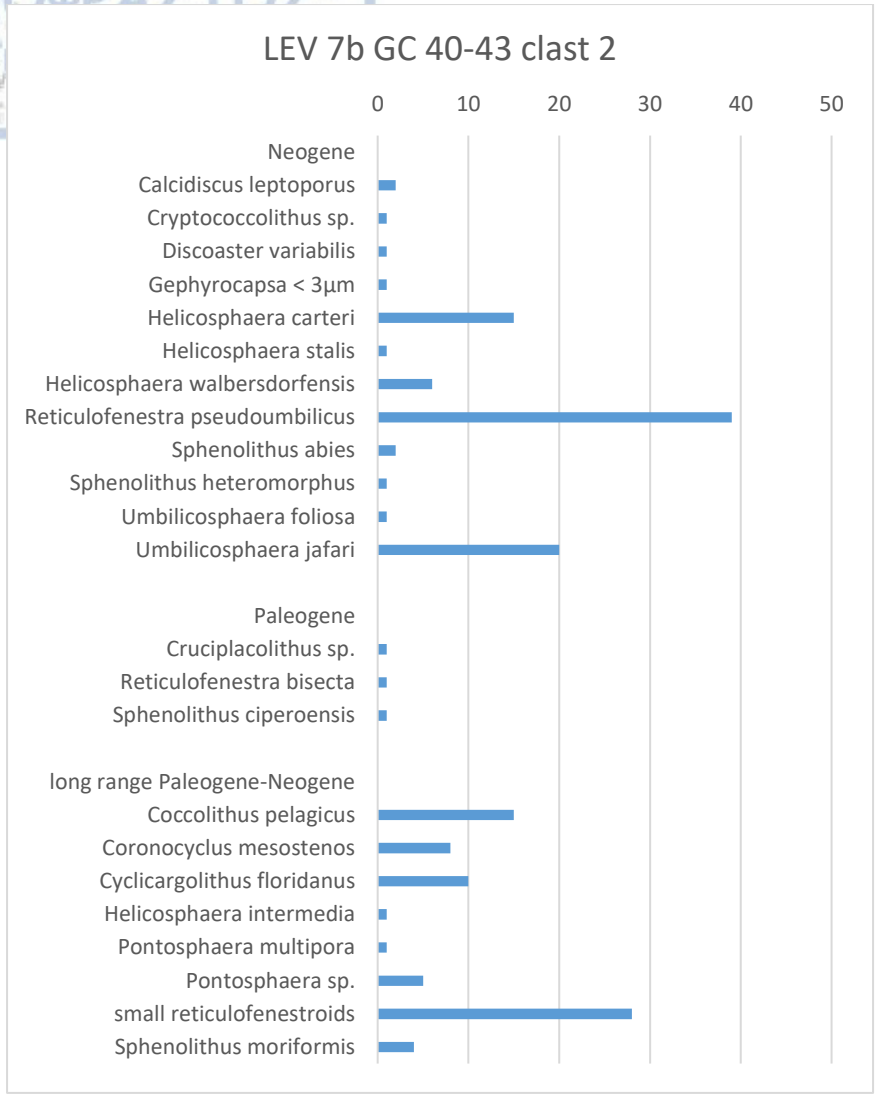

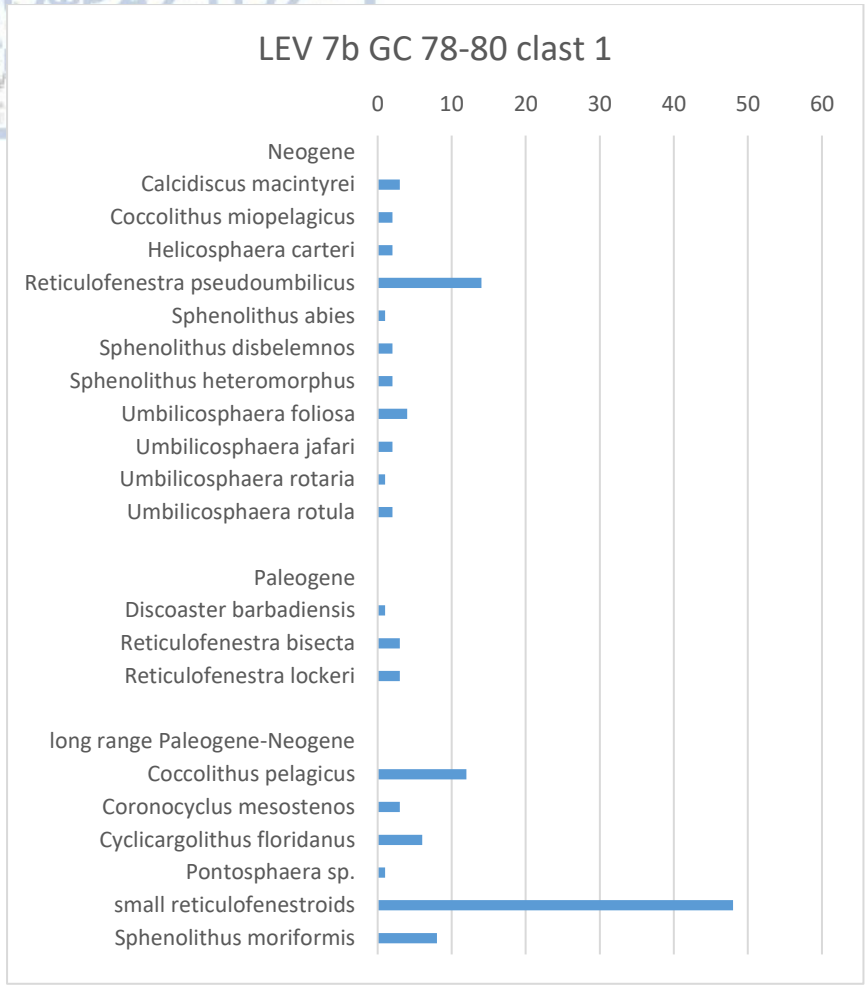

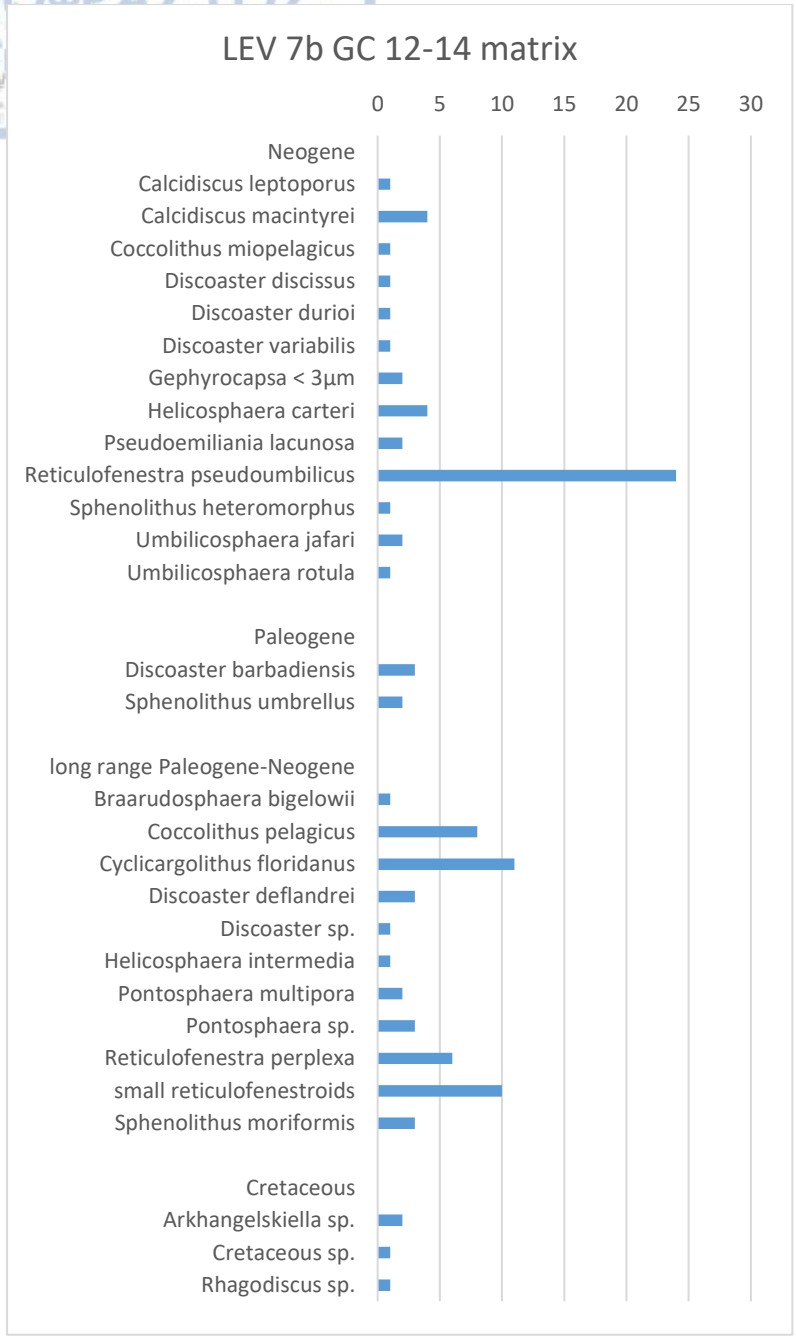

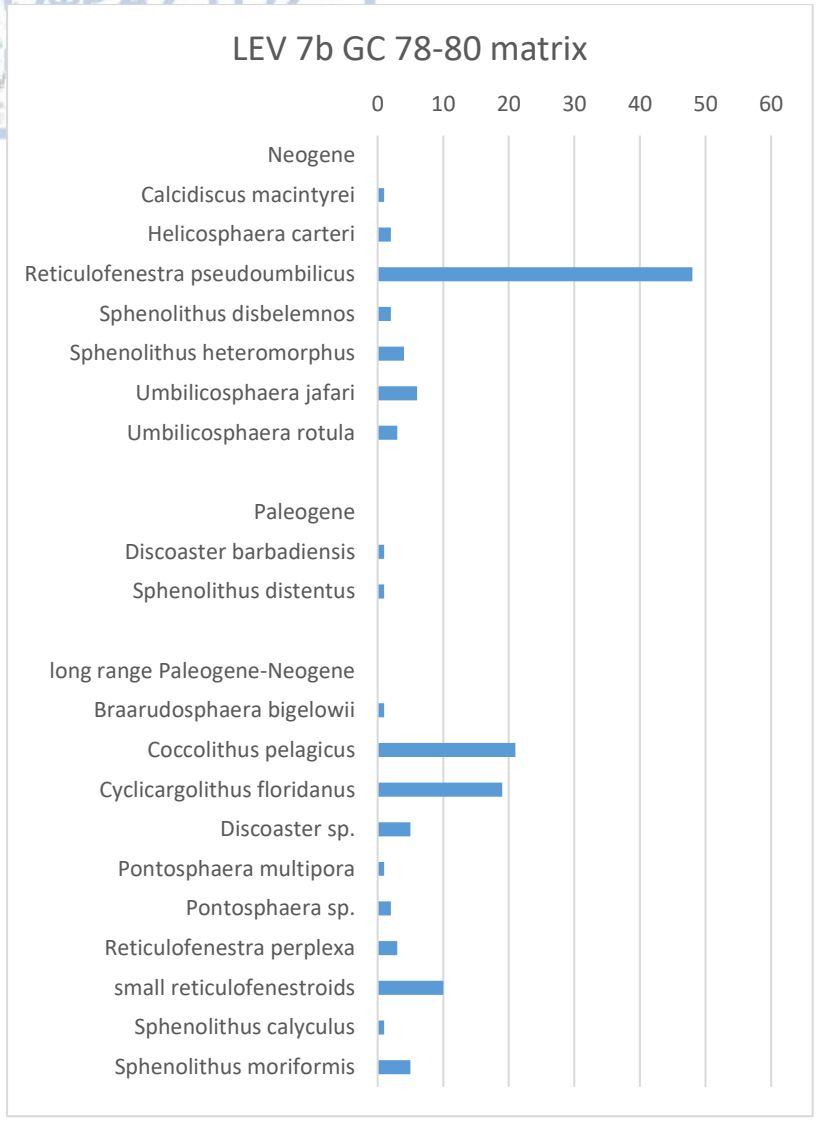

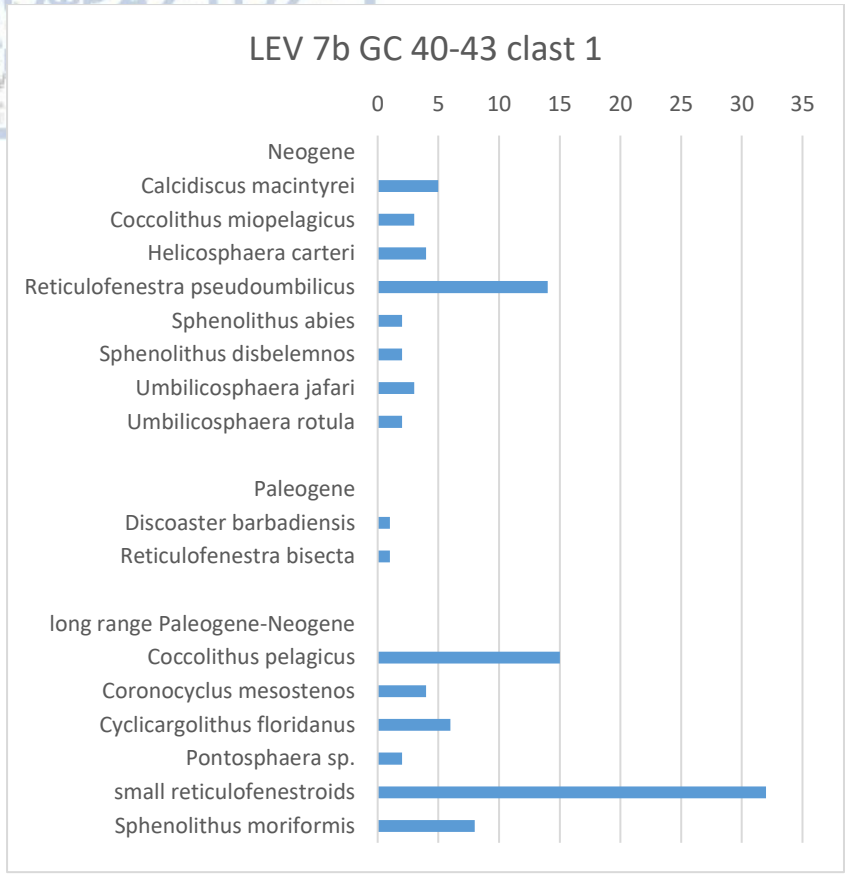

Leipzig MV

	MVs	interval (cm)	type	nanno (%)	Age	rock type	Consolidation	colour	comments	OI	HI	Tmax (°C)	TOC (%)	MINC (%)	S1 (mg/g)	S2 (mg/g)	S3 (mg/g)	carbonate content (%)
Leipzig	LEV 9b GC	10 - 13	*matrix*	30	Mixed Oligocene-Miocene	sandy mud		light yelowish brown	Quartz sound	224,62	52,31	428	0,65	1,52	0,01	0,34	1,46	12,12
	LEV 9b GC	10 - 13	clast 1	≤ 10	NN6	mudstone	well	dark grey-black		189,83	93,22	427	0,59	0,61	0,01	0,55	1,12	4,87
	LEV 9b GC	67 - 69	clast 1	< 10	NN4	mudstone	soft	light grey-grey		76,12	76,12	434	0,67	0,37	0,01	0,51	0,51	2,95
	LEV 9b GC	67 - 69	clast 2	almost barren	undetermined	sandstone	semi - well	greyish green		200,00	100,00		0,03	0,03	0,00	0,03	0,06	0,24
	LEV 9b GC	98 - 100	*matrix*	30	Mixed Oligocene-Miocene	sandy mud		light yelowish brown	Quartz sound	168,75	56,25	427	0,48	1,58	0,00	0,27	0,81	12,60
	LEV 9b GC	98 - 100	clast 1	≈ 10	Mixed Oligocene-Miocene	carbonate mudstone/ sandstone	semi - well	grey- dark/light grey	interbedding, quartz sound	207,69	42,31	424	0,26	9,35	0,00	0,11	0,54	74,58
	LEV 9b GC	98 - 100	clast 2	30-40	NN4	mudstone	semi - well	light grey-grey		127,59	63,22	424	0,87	3,58	0,00	0,55	1,11	28,55
	LEV 9b GC	98 - 100	clast 3	50-60	NN6	shale	well	light grey-grey	subparallel fissility	291,67	94,44	423	0,36	6,09	0,00	0,34	1,05	48,57
	LEV 9b GC	128 - 130	*matrix*	30	Mixed Oligocene-Miocene	sandy mud		light yelowish brown	Quartz sound	155,10	61,22	422	0,49	1,63	0,00	0,30	0,76	13,00
	LEV 9b GC	128 - 130	clast 1	?	undetermined	shale	semi - well	reddish brown	subparallel fissility	321,62	51,35	427	0,37	0,93	0,00	0,19	1,19	7,42
	LEV 9b GC	128 - 130	clast 2	20-30	NN5	carbonate mudstone	semi	yellowish greyish white		220,00	130,00	428	0,40	7,23	0,00	0,52	0,88	57,67
	LEV 9b GC	128 - 130	clast 3	≈ 5	NN6	?	?	?	?	73,33	64,00	426	0,75	0,26	0,00	0,48	0,55	2,07